Product Detection of the CH Radical Reactions with Ammonia and Methyl-Substituted Amines

Jérémy Bourgalais, Kacee L. Caster, Olivier Durif, David L. Osborn, Sébastien D. Le Picard, Fabien Goulay

Product Detection of the CH Radical Reactions with Ammonia and Methyl-Substituted Amines

Jeremy Bourgalais,[1] Kacee L. Caster,[2] Olivier Durif,[3] David L. Osborn,[4] Sebastien D. Le Picard,[3] and Fabien Goulay[2,*]

[1] *LATMOS/IPSL, UVSQ Université Paris-Saclay, Sorbonne Université, CNRS, Guyancourt, France*

[2]*Department of Chemistry, West Virginia University, Morgantown, West Virginia 26506, USA*

[3]*Astrophysique de Laboratoire, Univ Rennes, CNRS, IPR (Institut de Physique de Rennes) - UMR 6251, F-35000 Rennes, France*

[4]*Combustion Research Facility, Mail Stop 9055, Sandia National Laboratories, Livermore, California 94551, USA*

***Corresponding Author:** Fabien.Goulay@mail.wvu.edu

ABSTRACT

Reactions of the methylidyne (CH) radical with ammonia (NH_3), methylamine (CH_3NH_2), dimethylamine ($(CH_3)_2NH$), and trimethylamine ($(CH_3)_3N$), have been investigated under multiple collision conditions at 373 K and 4 Torr. The reaction products are detected using soft photoionization coupled to orthogonal acceleration time-of-flight mass spectrometry at the Advanced Light Source (ALS) synchrotron. Kinetic traces are employed to discriminate between CH reaction products and products from secondary or slower reactions. Branching ratios for isomers produced at a given mass and formed by a single reaction are obtained by fitting the observed photoionization spectra to linear combinations of pure compound spectra. The reaction of the CH radical with ammonia is found to form mainly imine, $HN=CH_2$, in line with an addition–elimination mechanism. The singly methyl substituted imine is detected for the CH reactions with methylamine, dimethylamine, and trimethylamine. Dimethylimine isomers are formed by the reaction of CH with dimethylamine, while trimethylimine is formed by the CH reaction with trimethylamine. Overall, the temporal profiles of the products are not consistent with the formation of amino carbene products in the reaction flow tube. In the case of the reactions with methylamine and dimethylamine, product formation is assigned to an addition-elimination mechanism similar to that proposed for the CH reaction with ammonia. However, this mechanism cannot explain the products detected by the reaction with trimethylamine. A C–H insertion pathway may become more probable as the number of methyl group increases.

1. INTRODUCTION

Ammonia and its amine derivatives are emitted as gases in the atmosphere from a variety of sources such as biomass burning, vegetation, combustion, as well as industry.[1,2] These nitrogen-containing molecules are of special interest in combustion environments where they impact the oxidation and ignition of hydrocarbon fuels.[3,4] In addition, their chemistry in reactive carbon-rich environments may play a significant role in the formation of NO_x.[5-10] An improved utilization of biomass-derived nitrogen-containing compounds as fuels and a better understanding of the role of amines in combustion both require a systematic study of the chemistry of ammonia and substituted amines with combustion relevant radicals.

A large number of experiments have been performed to investigate the reaction of ammonia with radicals such as OH, CN, C_2H, and CH.[11-15] Although its reaction with the OH radical is found to be slow ($<5\times10^{-13}$ cm^3 s^{-1} from 230 K to 450 K),[11] ammonia reacts at a significant fraction of the collision rate with the CN,[12] C_2H,[13] and CH radicals.[14] In the case of the reactions with OH and CN, the products are predicted to mostly be $NH_2 + H_2O$ and $NH_2 + HCN$.[13,16,17] The reaction with OH proceeds directly through a $HO–HNH_2$ abstraction saddle point,[16] while the reaction with CN initially forms a $NC–NH_3$ adduct that may rearrange and dissociate to form the final products.[13,17] The most exhaustive experimental and theoretical studies have been performed for the $CH + NH_3$ reaction.[15] The mechanism has been assigned as addition–elimination, as further described in this introduction. Kinetic investigations with methyl-substituted amines are scarcer and data are available only for reactions with OH and CH radicals.[14,18-22] Reactions with the OH radical proceed with a rate coefficient on the order of 1×10^{-11} cm^3 s^{-1} and are predicted to occur through interaction of the OH radical with an H-atom of both the amine and methyl groups to give the abstraction products.[18] Reactions of the CH radical with methyl substituted amines are fast ($>1\times10^{-10}$ cm^3 s^{-1})[14] although no mechanistic information is available.

The methylidyne (CH) radical is an important reactive intermediate detected in hydrocarbon flames (*e.g.,* methane, acetylene, ethene, ethane, propene, propane).[13,16,23,24] Its barrier-less addition toward a large number of organic and inorganic functional groups is due to the carbon atom having both one singly occupied and one empty non-bonding molecular orbital. Its formation in flames, along with other fuel-derived C_1-radicals (*e.g.*, CH_3, CH_2 and C), occurs primarily from oxidation of small hydrocarbon compounds (*e.g.,* methane, acetylene).[17,25] Once formed, the CH radical is likely to play a role in the formation of soot precursors through generation of small cyclic hydrocarbons.[23-28] A major interest of the CH radical in combustion is its ability to react with molecular nitrogen to form NCN, which is the dominant source of prompt NO formation in turbulent diffusion flames.[17,25-38] Its reaction with ammonia is also included in a recent combustion model.[25] As fuel complexity is increased, there is a need for additional data about the reaction of the CH radical with nitrogen containing hydrocarbons.

Zabarnick *et al.*[14] performed the first kinetic measurements of CH radical reactions with ammonia and methyl substituted amines. They employed pulsed laser photolysis (PLP) and laser-induced fluorescence (LIF) to measure rate constants for CH with NH_3, CH_3NH_2, $(CH_3)_2NH$ and $(CH_3)_3N$ at temperatures ranging from room temperature up to 677 K. Based on the observed large rate coefficients they suggested an insertion–elimination mechanism of CH into one of the N-H bonds followed by rapid dissociation of the energized complex. Bocherel *et al.*[39] measured the CH + NH_3 reaction also using a PLP–LIF technique in a supersonic flow reactor between 23 and 295 K. The reaction rate coefficient is 1.37×10^{-10} cm^3 s^{-1} at 295 K and displays no significant temperature (2.21×10^{-10} cm^3 s^{-1} at 23 K) or pressure dependences in agreement with the study of Zabarnick *et al.*[14] More recently Blitz *et al.*[15] investigated the products of the CH + NH_3 reaction by measuring the H-atom branching ratio using LIF. The close to unity H-atom branching ratio combined with high-level (MCSCF/CASSCF)

calculations[15] support an insertion–elimination mechanism similar to that proposed for the reactions of CH with saturated hydrocarbons.[40] In the case of ammonia the insertion is found to proceed first through the formation of a dative bond[15] between the carbon and the nitrogen atoms.[15]

The aim of the present study is to obtain a general mechanism for the reaction of CH with amines. For this purpose we present a systematic investigation of the products formed by reactions of ground state methylidyne CH($X^2\Pi$) radicals with NH_3 and three methyl derivatives: methylamine (MA) CH_3NH_2, dimethylamine (DA) $(CH_3)_2NH$, and trimethylamine (TA) $(CH_3)_3N$. To probe the reaction products, experiments are performed in a flow reactor under thermal conditions (373 K and 4 Torr) at the Advanced Light Source (ALS) synchrotron of Lawrence Berkeley National Laboratory (LBNL). Products sampled from the flow are detected using tunable vacuum ultraviolet (VUV) photoionization and time-of-flight mass spectrometry. Kinetic traces and photoionization spectra supported by thermodynamic and Franck−Condon factor calculations of the species have been used to infer the primary products of the reactions.

2. EXPERIMETAL PROCEDURE

The experiments are performed in a slow flow reactor coupled to a tunable VUV photoionization orthogonal acceleration time-of-flight mass spectrometer. A detailed description of the apparatus has been given in the literature[41-43] and only a brief description is given here. The reactions take place in a flow tube at 373 K and at a pressure of 4 Torr (total density ~10^{17} cm^{-3}). The 100 sccm gas flow consists of a large excess of He with 10% nitrogen and small amounts of CH-radical precursor (bromoform) and reagent gases (ammonia, MA, DMA, or TMA) with typical densities of ~10^{13} cm^{-3} and ~10^{14} cm^{-3} respectively. The bromoform ($CHBr_3$) is placed in a glass vessel and its vapor carried into the main carrier gas flow by bubbling a controlled flow of He through the liquid. The purities of gases are:

bromoform (99%), $CDBr_3$ (≥99%, ≥99.5 atom % D), NH_3 (≥99.9%), CH_3NH_2 (≥99%), $(CH_3)_2NH$ (≥99%), $(CH_3)_3N$ (≥99%).

CH radicals are generated by excimer laser photolysis at 248 nm with a 4 Hz repetition rate. The laser power output is typically 266 mJ per pulse for a 20 ns pulse duration, with a photolysis fluence inside the flow tube of ~20−50 mJ cm^{-2}. Photodissociation occurs via successive absorption of photons eliminating multiple halogen atoms leading to CH number density of about 2.5×10^{10} cm^{-3} in the reaction flow.[44,45]

The gas mixture is sampled through a pinhole halfway down the flow tube into a high-vacuum chamber. A skimmer generates a molecular beam into the ionization chamber where species are ionized by the quasi-continuous tunable VUV synchrotron radiation of the ALS. The formed ions are detected through time-of-flight mass spectrometry by recording their arrival time with respect to the extraction pulse and laser pulse. The setup leads to complete time- and energy-resolved mass spectra by averaging 200-500 laser pulses for each ionizing photon energy. The photoionization spectra are obtained from three independent data sets, averaged and integrated, over the mass-to-charge ratio and time window of interest. In the following sections a time window up to 80 ms was interrogated after the laser pulse. Mass spectra, kinetic time traces, and photoionization spectra are corrected for pre-photolysis signals by subtracting the average ion counts in a 20 ms time window before the laser pulse. Having subtracted this time-independent signal, the data in the figures represents the change of signals as a result of the reactive species created by the laser pulse. Positive signals represent species created because of the laser pulse, whereas negative signals correspond to species that are depleted following irradiation. Finally, all signals are normalized to variations in VUV photon flux that is monitored using a calibrated photodiode.

3. COMPUTATIONAL METHODS

Electronic structure calculations of neutral species and their cations leading to their optimized geometries have been performed using the Gaussian09 package with the B3LYP/CBSB7 method. Details about the calculations have been discussed elsewhere.[41,42,46,47] Heats of reaction, and adiabatic and vertical ionization energies, are calculated using the CBS-QB3 composite method.[48,49] Simulated Franck−Condon factors of isomer species are calculated at room temperature with the G09 package within the Franck−Condon approximation.[44,50] Although the experiments are performed at 373 K, the higher temperature does not result in significantly different vibrational populations. The calculated Franck−Condon factors are convolved with a Gaussian response function (FWHM of 0.025 eV) and integrated in order to simulate the photoionization spectra of the species assuming that direct ionization dominates the ionization process.

Saddle points for H- and CH_3-transfer on the CH + CH_3NH_2 potential energy surface (PES) are calculated using the CBS-QB3 composite method.[48,49] The saddle points are verified with intrinsic reaction coordinate (IRC) calculations at the B3LYP/6-31G(d) level of theory.

4. RESULTS

Under the present experimental conditions (4 Torr, 373 K, high dilution with inert gases), collisional quenching with the He (90%) and N_2 (10%) buffer gases will rapidly thermalize all the photolysis and reaction products to the temperature of the flow. Stabilization will not compete with dissociation of the reaction intermediates as long as the unimolecular dissociation occurs with a rate higher than the collision rate ($<20 \times 10^6$ s^{-1}). All the initial reaction adducts formed by addition of the CH radicals with unsaturated hydrocarbons are expected to have lifetimes shorter or on the order of their rotational period.[40] Assuming equally fast adduct isomerization and dissociation for reactions with amines under the above experimental conditions, stabilization of these intermediates through collisional quenching is not expected

to be a significant process. For these reasons, performing the experiments under thermal conditions provides information about the unimolecular isomerization and dissociation scheme of the reaction intermediates.

The kinetic traces and photoionization spectra are recorded by irradiating a mixture of $CHBr_3$ and the chosen amine in a He/N_2 mixture at 248 nm. Along with CH($X^2\Pi$, v=0), bromoform photodissociation produces CH($A^2\Delta$), CH($X^2\Pi$, v=1), Br, HBr, CBr, CHBr, Br_2 and $CHBr_2$. The CH($A^2\Delta$) population decays radiatively within few microseconds after the laser pulse.[51] The vibrationally excited CH($X^2\Pi$, v=1) radicals are efficiently quenched by adding nitrogen to the main flow.[28,52] The three body reaction of the CH ($X^2\Pi$, v=0) radical with molecular nitrogen is slow[53] at the pressure of the flow and is unlikely to affect the observed product distributions. Reactions of CBr with small unsaturated hydrocarbons are several orders of magnitude slower at the present temperature[46,47,50,54-56] than those for reactions of the CH radical.[54,55,57,58] Similarly slow kinetics between CBr and amines would allow discriminating between CBr and CH reaction products. At 248 nm the singlet CHBr carbene is expected to be formed in very low concentrations compared to the CH radical.[59] Its reaction with ammonia or the methyl-substituted amine reactants may form products through HBr-loss at the same m/z as the CH reaction products. There are no kinetic data available for the reactions of halocarbenes with amines. In the case of reactions with DMA and TMA, signals are observed at m/z values corresponding to dimethyl and trimethyl substituted amines plus $C^{79}Br/C^{81}Br$ isotopes. This indicates that the methyl substituted amines reacts with CBr to give the stabilized adduct, or with CHBr followed by a H-loss. The detection of brominated products suggests that the branching ratio for Br and/or HBr elimination is less than unity. Combined with the non-detection of signal at the m/z values of the brominated radicals, this suggests that the direct contribution of the CBr and CHBr reactions to signals at m/z corresponding CH reaction products is therefore expected to be small.

Successive reactions of the primary products with remaining radicals in the flow may lead to the formation of secondary products over the experimental reaction time. Because the reactions of CH with ammonia and amines are very fast,[14] it is possible to discriminate between primary and secondary reactions by inspecting the product temporal profiles. Figure S1 displays typical kinetic traces obtained when irradiating a mixture of bromoform and MA in helium and nitrogen. The fast rise of the signals at m/z 42, 43, and 57 indicates that these products are likely to be formed by a fast reaction while the slower rise observed at m/z 58 suggests that the corresponding product is from a slower or secondary reaction. In this section photoinzation spectra are integrated over the 0–40 ms time range, whereas mass spectra integrations are restricted to 0–5 ms in order to minimize contribution from secondary or slower reactions. Products showing initial formation rates of less than 500 s^{-1} are assigned to secondary reactions and are not discussed further.

Time- and energy-resolved mass spectra are recorded by averaging at least 500 laser shots at each VUV photon energy, scanned over at least 1.5 eV with an energy step of 25 meV. Ar is used in a gas filter in order to absorb harmonics of the undulator radiation. All the amines used in this work have low absorption cross-sections at 248 nm ($<1\times10^{-19}$ cm^2 for MA and DMA, $\sim1\times10^{-18}$ cm^2 for TMA)[60-62] leading to negligible dissociation of MA and DMA and less 6% dissociation for TMA. Nonetheless, mass spectra of the NH_3, MA, DMA where systematically recorded with and without bromoform in order to confirm that no time-dependent signal was observed at the masses of the expected CH + amine reaction products. Although no background was recorded in the case of TMA, time resolved signal observed at m/z 58 is attributed to TMA photodissociation.

In the following sections, isomer products are identified based on their ionization energy and photoionization spectra. When experimental values are not available, the isomers are identified using the CBS–QB3 calculated ionization energies displayed in Table 1. The

difference of ionization energies between the C_2H_5N cis and trans stereoisomers is found to be less than 0.02 eV and the isomer identification is performed using the trans isomer. The photoion spectra are also fit with integrated experimental or integrated calculated (Franck–Condon factors) photoelectron spectra. The predicted spectra for individual isomers are displayed in Figure S1 (supplementary information). The integrated photoelectron spectra[63] do not distinguish between the cis and trans stereoisomers. The photoelectron spectra for the methyl substituted imines are integrated over the first two vibronic bands of the cation[63] and normalized to their maximum. Because of the large uncertainties in absolute photoionization cross sections between the different mass channel products, the data are not used to provide reaction product branching fractions. Nonetheless, isomeric branching ratios for a given mass channel are estimated on the assumption that isomers have equal ionization cross sections.[64] In the following paragraphs the displayed photoionization spectra for the individual isomers are weighted by their branching ratios.

Table 1. Ioniczation energies of imines and amino carbene isomers calculated using the CBS–QB3 method

		Imines RN=CR'R"				Amino carbene RR'N–CR"			
Formula	m/z	Isomer	IE (eV)	Isomer	IE (eV)	Isomer	IE (eV)	Isomer	IE (eV)
CH_3N	29		9.94				8.39		
C_2H_5N	43	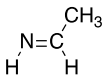	9.54[(1)]	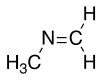	9.13	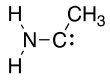	7.65	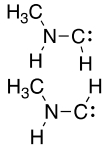	7.88 7.84
C_3H_7N	57	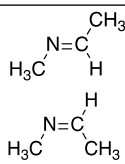	8.83 8.67	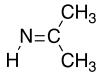	9.19	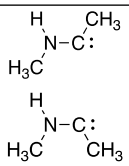	7.38 7.18	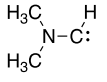	7.53
C_4H_9N	71	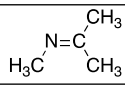	8.42			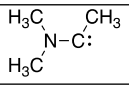	6.91		

[(1)]Cis and trans isomers

4.1 CH + NH_3

Two H-loss exit channels of the CH + NH_3 reaction (R1) are possible, producing the imine $HN{=}CH_2$ and the amino carbene $H_2N{-}CH$ through channels R1a and R1b, respectively. The only other exothermic reaction exit channel predicted by Blitz *et al.*[15] is the formation of CH_3 + NH.

CH + NH_3 →	$HN{=}CH_2$ + H	-244.44 kJ.mol^{-1}	R1a
	$H_2N{-}CH$ + H	-94.96 kJ.mol^{-1}	R1b
	CH_3 + NH	-29.4 kJ.mol^{-1}	R1c[15]

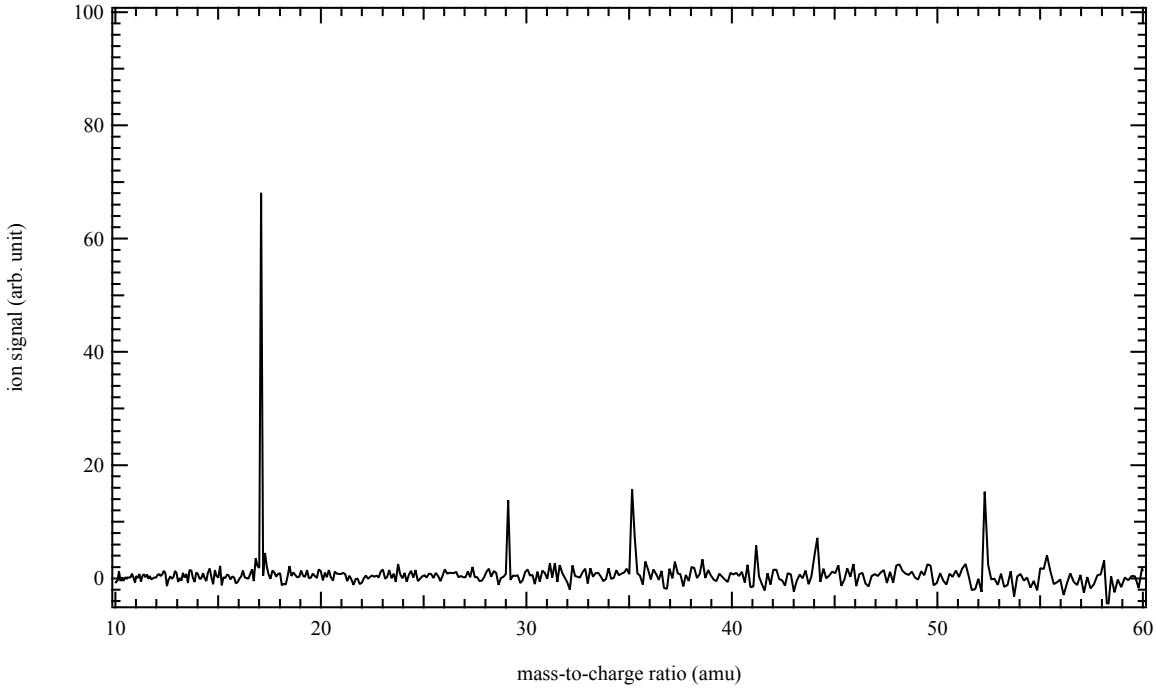

Figure 1. Mass spectrum obtained by photolysis of a $CHBr_3$ and NH_3 mixture in helium and nitrogen integrated over the 9.8-10.6 eV photon energy and the 0–5 ms time range.

Figure 1 displays the mass spectrum obtained by photolysis of a $CHBr_3$ and NH_3 mixture in helium integrated over the 9.8-10.6 eV photon energy and the 0–5 ms time range. The large signal at m/z 17 is likely due to fluctuations in the ammonia signal leading to a remaining positive signal after background subtraction. The main signals are observed at m/z 29, 35, and 52. The signal at m/z 29 displays a fast rise immediately after the laser pulse, as expected for a

CH + NH_3 reaction product. The temporal profiles of m/z 35 and 52 show a sharp signal rise starting about 4 ms after the laser pulse and displaying a rapid decay over the following 5 ms. Although the origin of these two signals is undetermined, NH_3•H_2O and $2NH_3$•H_2O are the only species that match the observed m/z values. The formation of these clusters at 373 K is not favorable and the observed ions are more likely to come from dissociative ionization of higher mass neutral species. Additional signals (not shown here) are observed at m/z 79, 81, 104, and 106 corresponding to Br atoms and brominated compounds. The photoion signal at m/z 104 and 106 has a fast kinetic rise and shows an ion onset at about 10.3 eV corresponding to the photoionization energy of bromoacetylene.[65] Although there is no clear pathway leading to BrCCH formation in the reaction flow, its formation does not interfere with the detection of CH + NH_3 products. From this analysis, it is concluded that only the signal at m/z 29 originates from the CH + NH_3 reaction.

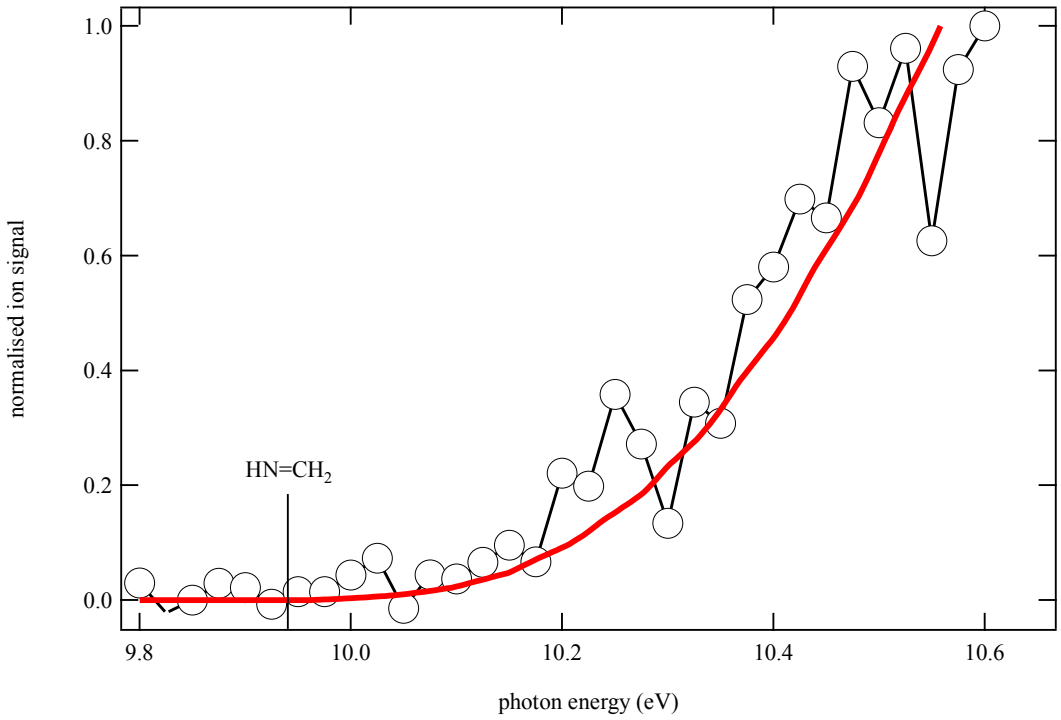

Figure 2. Photoionization spectrum of m/z 29 (open circles) obtained by photolysis of a $CHBr_3$ and NH_3 mixture in helium and nitrogen integrated over the 0–40 ms time range and displayed from 9.8 to 10.6 eV photon energy. The vertical line denotes the experimental ionization energy

of $HN=CH_2$.[63] The thick red line is the integrated experimental photoelectron spectrum of $HN=CH_2$ from Bock *et al.*[63]

Figure 2 displays the photoionization spectrum of m/z 29 integrated over the 0−40 ms time range. The good match between the experimental data (open circles) and the integrated experimental photoelectron spectrum of $HN=CH_2$ (red thick line) from Bock *et al.*[63] confirms the formation of $HN=CH_2$ in the reaction flow. As displayed in Table 1 the calculated H_2N–CH amino carbene ionization energy is 8.39 eV, well below that of the $HN=CH_2$ isomer. The absence of signal below 9.9 eV confirms that the amino carbene isomer H_2N–CH is not formed in the reaction flow and that only R1a contributes to the reaction mechanism. Additional experiments were performed with deuterated bromoform as the radical precursor in order to provide information on isomerization pathways. The main CD + NH_3 product signal is observed at m/z 30 with no significant signal at m/z 29, indicating an absence of D loss from the initial adduct. The photoionization spectrum of m/z 30 is identical to that of m/z 29 from the CH + NH_3 reaction.

4.2 CH + CH_3NH_2

The reaction of the CH radical with MA (R2) may proceed both by H- (R2a, b, c, and d) or CH_3-loss (R2e and f) to form imines (R2a, b, and e) or amino carbenes (R2c, d, and f) at m/z 43 and 29. The enthalpy of reaction for producing trans- vs. cis-$HN=CHCH_3$ or trans- vs. cis-CH_3HN–CH stereoisomers differs by less than 3 kJ mol^{-1}; the enthalpies of reaction given in R2a and R2c are for the trans isomers. All the exit pathways are exothermic with formation of the imines being at least 100 kJ.mol^{-1} more exothermic than the amino carbenes.

$CH + CH_3NH_2 \rightarrow$	$HN=CHCH_3$ (m/z 43)	+	H	-313.17 kJ.mol^{-1}	R2a
	$CH_3N=CH_2$ (m/z 43)	+	H	-277.36 kJ.mol^{-1}	R2b
	CH_3HN–CH (m/z 43)	+	H	-128.99 kJ.mol^{-1}	R2c
	H_2N–CCH_3 (m/z 43)	+	H	-168.82 kJ.mol^{-1}	R2d

$HN{=}CH_2$	(m/z 29)	+	CH_3	-251.30 kJ.mol^{-1}	R2e
$H_2N{-}CH$	(m/z 29)	+	CH_3	-101.82 kJ.mol^{-1}	R2f

Figure 3 displays the photoionization spectrum of m/z 29 (open circles) obtained by photolysis of a $CHBr_3$ and CH_3NH_2 mixture in helium and nitrogen integrated over the 0−40 ms time range. The thick red line is the integrated photoelectron spectrum of $HN{=}CH_2$ from Bock *et al.*[63] The good match between the experimental data and the integrated photoelectron spectrum as well as the absence of signal below 9.9 eV suggest that only the imine isomer is formed in the reaction flow.

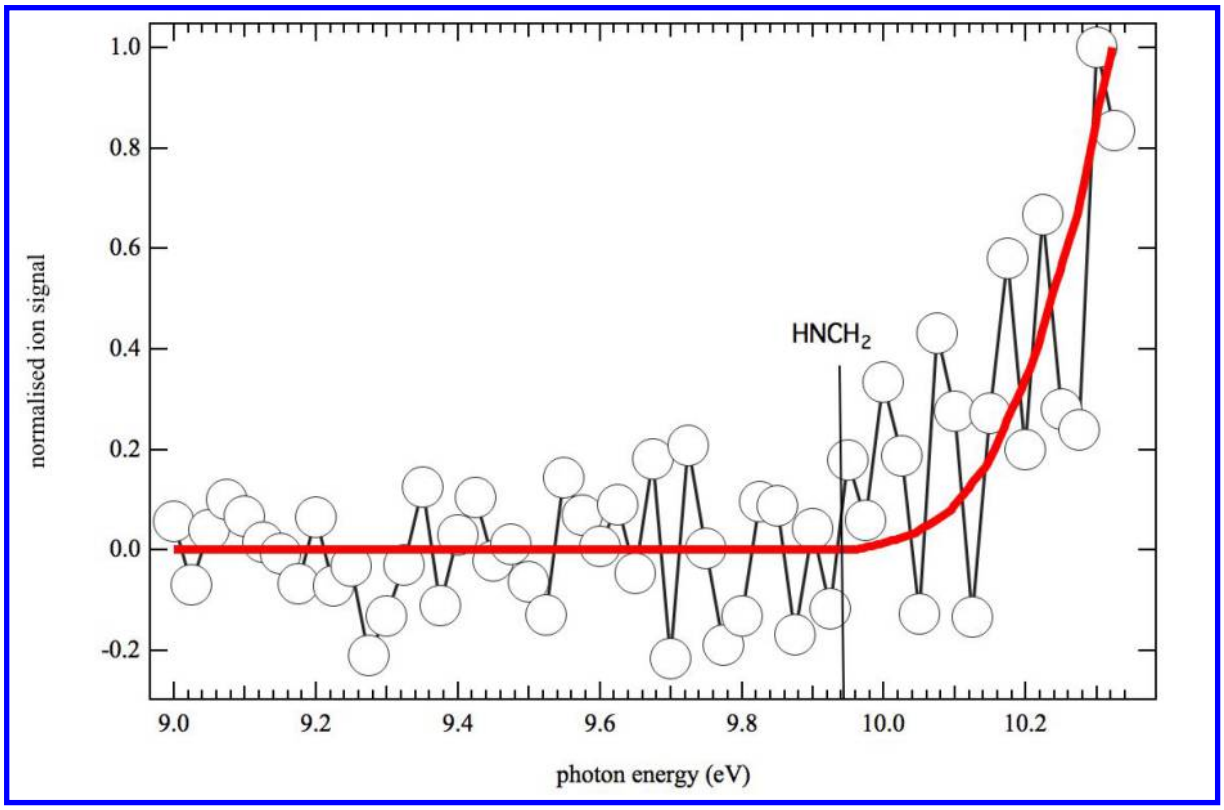

Figure 3. Photoionization spectrum of m/z 29 (open circles) obtained by photolysis of a $CHBr_3$ and CH_3NH_2 mixture in helium and nitrogen integrated over the 0−40 ms time range and displayed from 9.0 to 10.3 eV photon energy. The thick red line is the integrated photoelectron spectrum of $HN{=}CH_2$ from Bock *et al.*[63]

Figure 4 displays the photoion signal at m/z 15 (open circles) integrated over the 0–40 ms time range obtained by photolysis of a $CHBr_3$ and CH_3NH_2 mixture. The data is superposed to the

experimental spectrum of the methyl radical (red line).[66] The good match confirms the formation of CH_3 radical in the reaction flow.

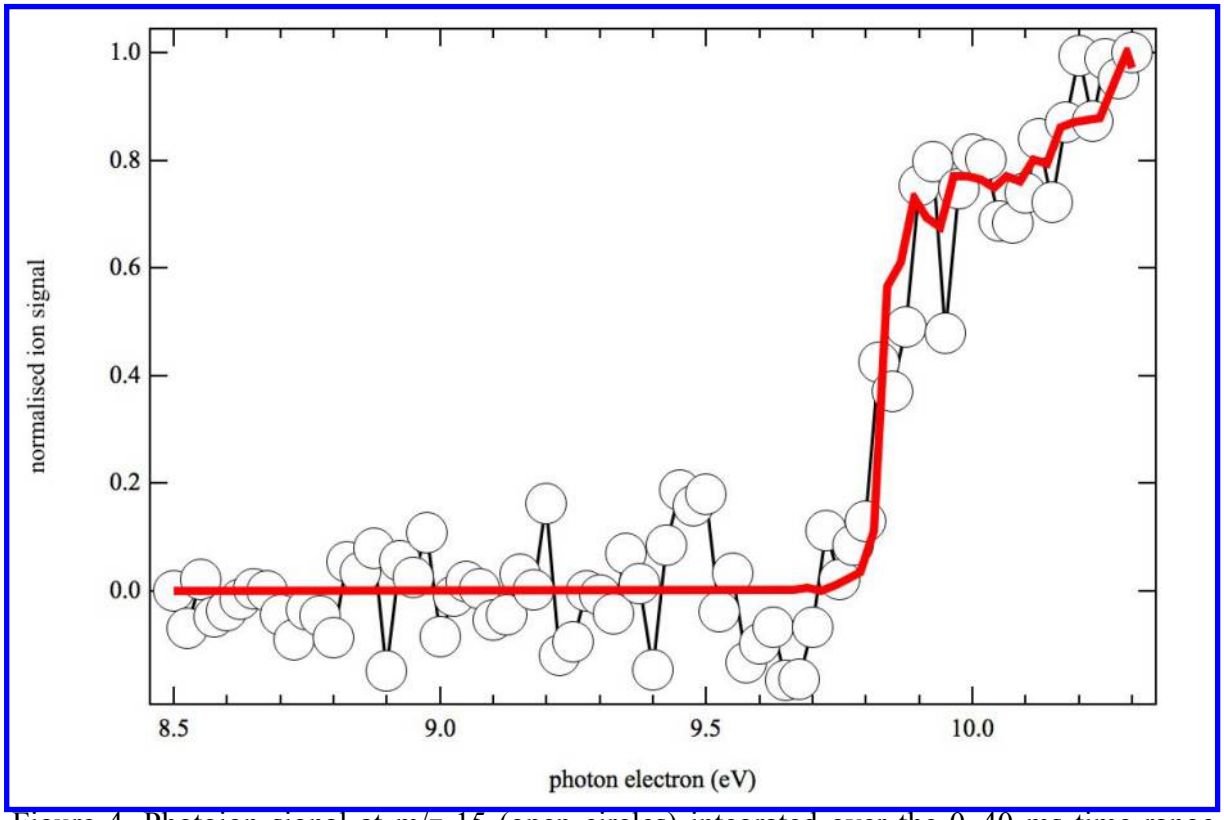

Figure 4. Photoion signal at m/z 15 (open circles) integrated over the 0–40 ms time range obtained by photolysis of a $CHBr_3$ and CH_3NH_2 mixture in helium and nitrogen displayed from 8.5 to 10.3 eV photon energy. The thick red line is the absolute spectrum (solid red line) of the methyl radical (CH_3) obtained by Savee *et al.*[66]

Figure 5 displays the photoionization spectra obtained at m/z 43 recorded under the same experimental conditions as those of Figures 3 and 4. The purple solid line is a fit to the data using normalized integrated photoelectron spectra of two methylimine isomers: $CH_3N{=}CH_2$ (blue dashed line) and $HN{=}CHCH_3$ (red dotted line),[63] assuming equal photoionization cross sections after the first two vibronic bands. The fit to the data returns a $CH_3N{=}CH_2$:$HN{=}CHCH_3$ branching ratio of 0.9:1. The absence of onset at the ionization energy of the $CH_3N{=}CH_2$ is likely due to the poor Franck–Condon overlap between the neutral and cation vibronic ground states.

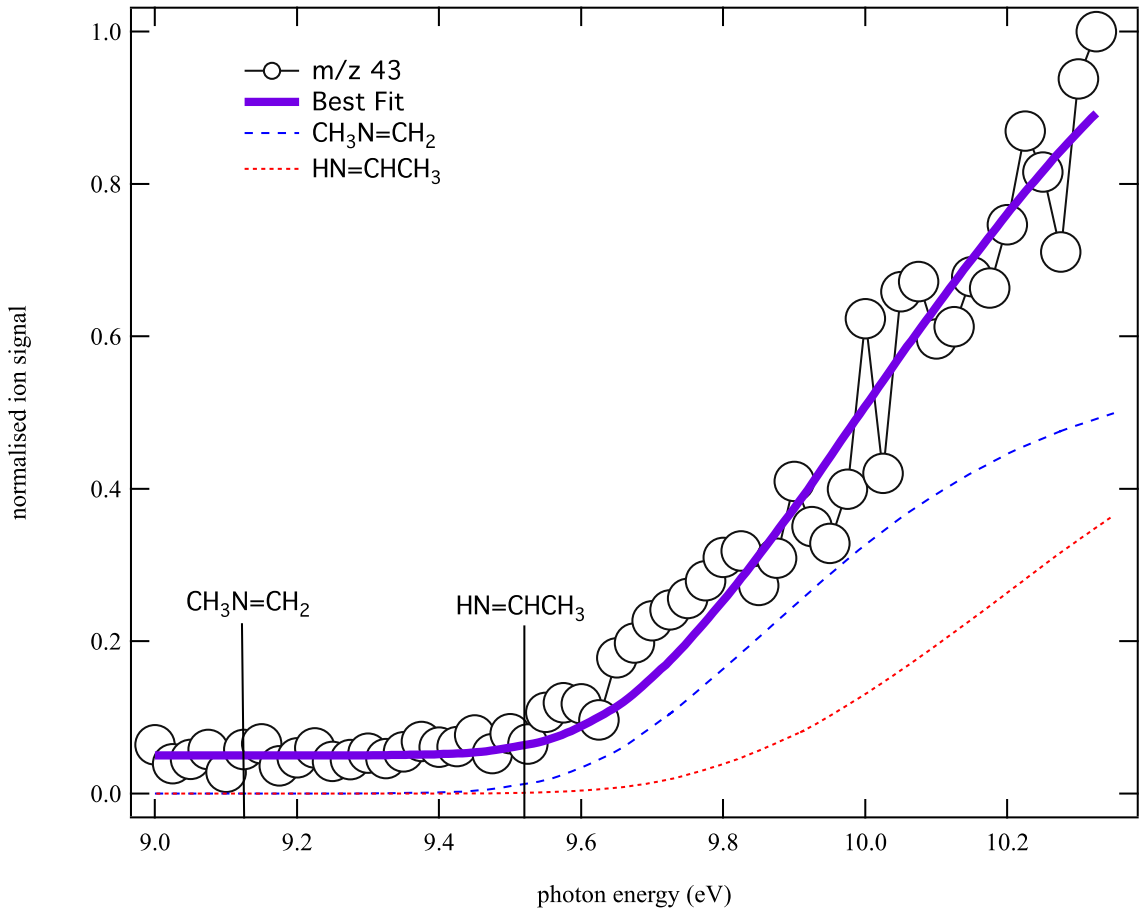

Figure 5. Photoionization spectrum at m/z 43 (open circles) obtained by photolysis of a $CHBr_3$ and CH_3NH_2 mixture in helium and nitrogen integrated over the 0−40 ms time range. The purple solid line is a fit to the data using the integrated photoelectron spectra of $CH_3N{=}CH_2$ (blue dashed line), $HN{=}CHCH_3$ (red dotted line) from Bock *et al.*[63] The best fit to the data is obtained for a $CH_3N{=}CH_2$:$HN{=}CHCH_3$ branching ratio of 0.9:1.

In Figure 5, a small ion signal is observed from 9.0 – 9.1 eV, below the energy of both imine isomers. Inspection of the kinetic traces reveals that the corresponding ions are detected only after irradiation of the flow by the laser pulse. This signal below 9.1 eV remains constant after the laser pulse, which is uncharacteristic of reactive carbene molecules. No signals are detected at the m/z corresponding to the brominated adducts, and the offset is therefore unlikely to be due to dissociative ionization of higher mass products. The constant signal offset below the energy of the methylimine isomers does not enable us to unequivocally rule out the

formation of the amino carbene isomers, but should not affect the methylimine branching ratios.

4.3 CH + $(CH_3)_2NH$

The reaction of the CH radical with dimethyl amine may lead to a total of 8 exothermic exit channels, through H-loss (R3a, a' b, c, and d) and CH_3-loss (R3e, f, g, and h). The enthalpy in R3e is for the trans isomer. As for the reaction with MA, formation of the methyl amino carbenes (R3c, d, g, and h) is found to be less thermodynamically favorable by at least 100 $kJ.mol^{-1}$.

CH + $(CH_3)_2NH$ →	*trans*-$CH_3N{=}CHCH_3$	(m/z 57)	+	H	-325.18 $kJ.mol^{-1}$	R3a
	cis-$CH_3N{=}CHCH_3$	(m/z 57)	+	H	-309.193 $kJ.mol^{-1}$	R3a'
	$HN{=}C(CH_3)_2$	(m/z 57)	+	H	-358.53 $kJ.mol^{-1}$	R3b
	trans-$CH_3HN{-}CCH_3$	(m/z 57)	+	H	-181.70 $kJ.mol^{-1}$	R3c
	cis-$CH_3HN{-}CCH_3$	(m/z 57)	+	H	-161.38 $kJ.mol^{-1}$	R3c'
	$(CH_3)_2N{-}CH$	(m/z 57)	+	H	-142.55 $kJ.mol^{-1}$	R3d
	$HN{=}CHCH_3$	(m/z 43)	+	CH_3	-300.33 $kJ.mol^{-1}$	R3e
	$CH_3N{=}CH_2$	(m/z 43)	+	CH_3	-264.53 $kJ.mol^{-1}$	R3f
	trans-$CH_3HN{-}CH$	(m/z 43)	+	CH_3	-116.16 $kJ.mol^{-1}$	R3g
	cis-$CH_3HN{-}CH$	(m/z 43)	+	CH_3	-112.52 $kJ.mol^{-1}$	R3g'
	$H_2N{-}CCH_3$	(m/z 43)	+	CH_3	-155.99 $kJ.mol^{-1}$	R3h

Figure 6 displays the mass spectrum obtained by photolysis of a $CHBr_3$ and $(CH_3)_2NH$ mixture in helium and nitrogen integrated over the 8.5-10.6 eV photon energy and the 0–5 ms time range. The main signals are detected at m/z 15, 42, 43, 57 and 58. The signal at m/z 58 increases more slowly (400 s^{-1}) than the other signals and is likely not a direct product of the CH + DMA reaction. The photoion spectrum of m/z 42 shows an ionization onset at ~9.7 eV with a photoionization spectrum characteristic of propene (C_3H_6).

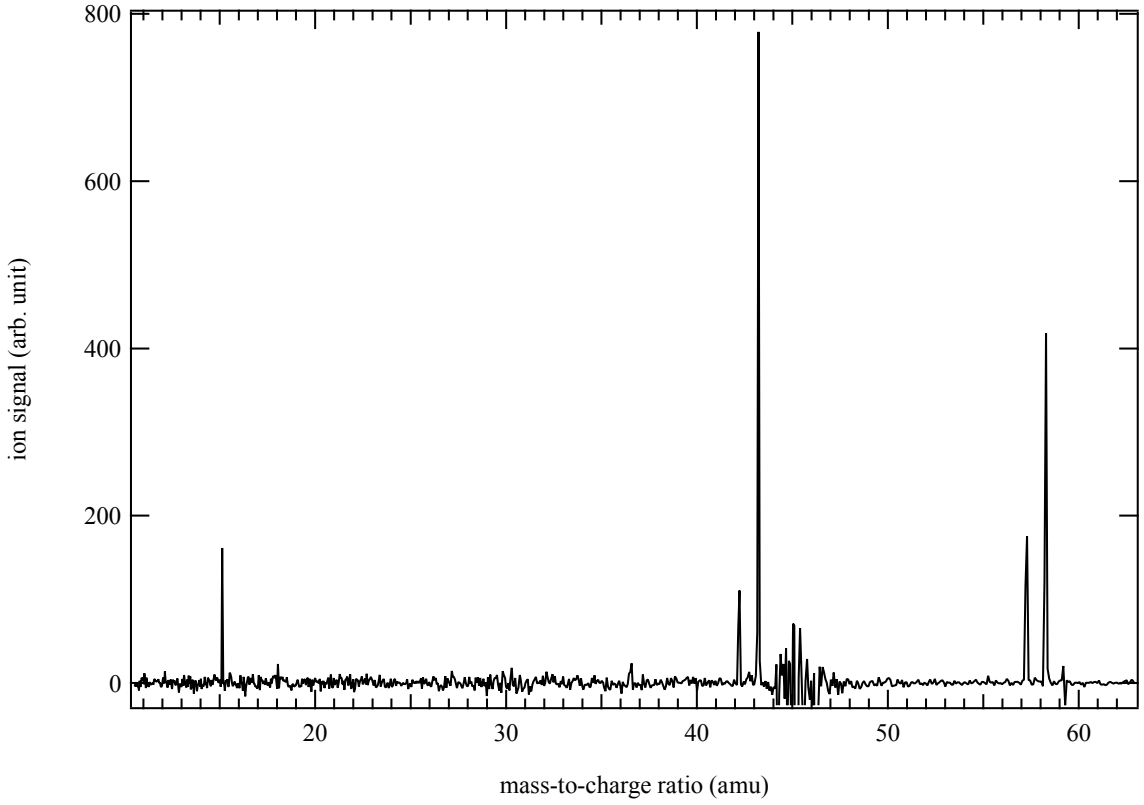

Figure 6. Mass spectrum obtained by photolysis of a $CHBr_3$ and $(CH_3)_2NH$ mixture in helium and nitrogen integrated over the 8.5-10.6 eV photon energy and the 0–5 ms time range.

Figure 7 displays the photoion signal at m/z 43 (open circles) integrated over the 0–40 ms time range from the same experiment. The purple solid line is a fit to the data using the integrated photoelectron spectra of $CH_3N{=}CH_2$ (blue dashed line) and $HN{=}CHCH_3$ (red dotted line) from Bock *et al.*[63] The best fit to the data is obtained for a $CH_3N{=}CH_2$:$HN{=}CHCH_3$ ratio of 0.7:1. No ion signal is detected at low energy, suggesting that no methyl amino carbene isomers are formed. The excepted mass 43 co-product, the methyl radical, is detected at m/z 15 with a photoionization spectrum identical to that displayed in Figure 4.

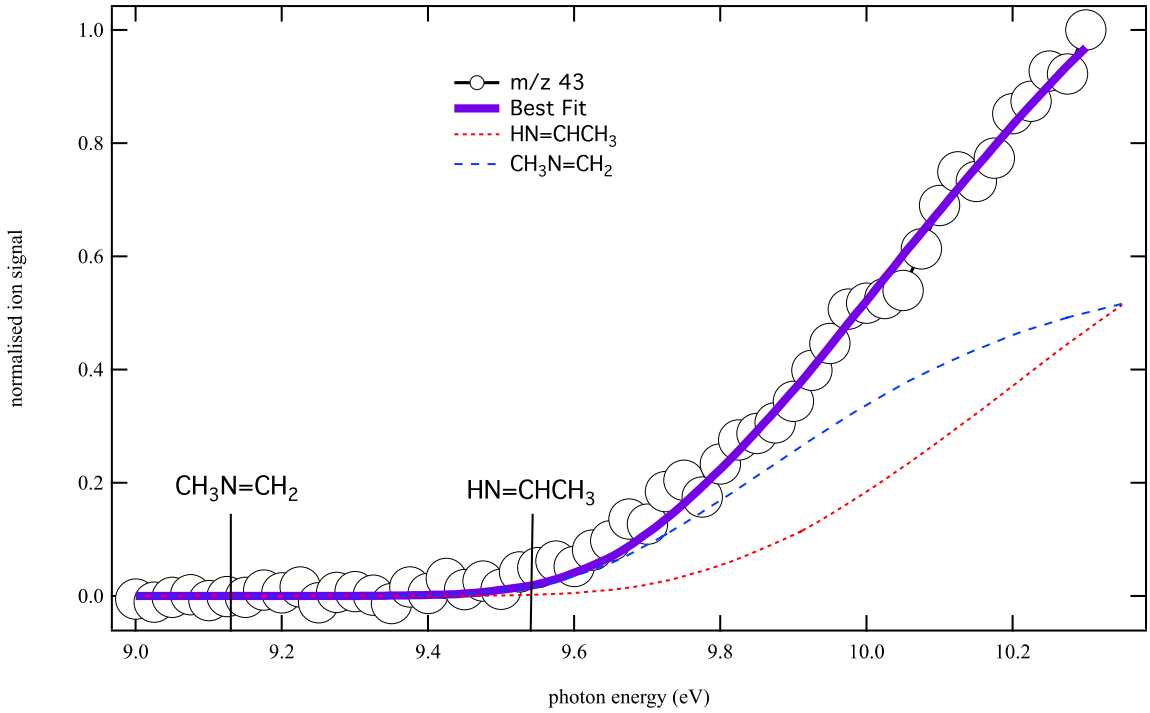

Figure 7. Photoionization spectrum at m/z 43 (open circles) obtained by photolysis of a $CHBr_3$ and $(CH_3)_2NH$ mixture in helium and nitrogen integrated over the 0−40 ms time. The purple solid line is a fit to the data using the integrated photoelectron spectra of $CH_3N{=}CH_2$ (blue dashed line) and $HN{=}CHCH_3$ (red dotted line) from Bock *et al.*[63] The best fit to the data is obtained for a $CH_3N{=}CH_2$:$HN{=}CHCH_3$ branching ratio of 0.7:1.

Figure 8 displays the photoionization spectrum at m/z 57 (open circles) recorded under the same experimental conditions as those of Figure 6 and 7. The purple solid line is a fit to the data using the integrated photoelectron spectra of $HN{=}C(CH_3)_2$ (red dashed line) from Bock *et al.*[63] as well as integrated Franck-Condon factors for the trans- (blue dotted line) and cis- (blue dotted and dashed line) $CH_3N{=}CHCH_3$ isomers. There is a constant signal offset below the ionization energies of the cis and trans dimethylimine stereoisomers. Although the observed signal could be attributed to the dimethyl amino-carbenes $CH_3HN{-}CCH_3$ and $(CH_3)_2N{-}CH$, the m/z 57 temporal profile below the energy of the $CH_3N{=}CHCH_3$ dimethylimine isomers displays a constant signal after its formation by the laser pulse. Such time-trace is unlikely for reactive carbene compounds. Signals are also detected at m/z 121/123, 122/124 and 135/137,

likely corresponding to brominated compounds. No signals are observed at m/z 136/138 or 137/139 values corresponding to the CHBr/CBr + DMA reaction adducts. Dissociative ionization of singly brominated products through HBr or H loss is therefore not likely to explain the observed signal offset. Alternatively, the offset could be due to dissociative ionization of CBr_2 reaction adducts through Br_2 loss. The best fit to the data using a constant offset before the ionization energy of the $CH_3N{=}CHCH_3$ dimethylimine isomers returns a trans-$CH_3N{=}CHCH_3$:cis-$CH_3N{=}CHCH_3$:$HN{=}C(CH_3)_2$ of 1:0.2:0.8.

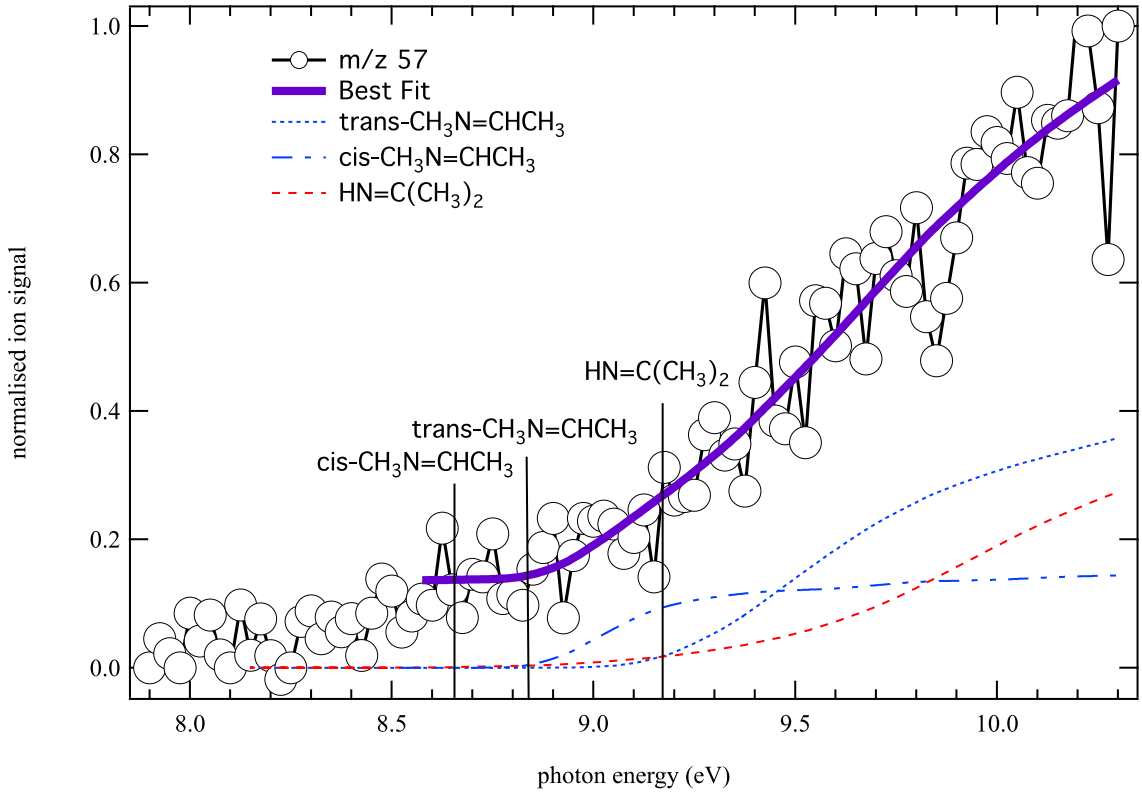

Figure 8. Photoion signal at m/z 57 (open circles) obtained by photolysis of a $CHBr_3$ and $(CH_3)_2NH$ mixture in helium and nitrogen integrated over the 0−40 ms time range and displayed from 7.8 to 10.2 eV photon energy. The purple solid line is a fit to the data using the integrated photoelectron spectra of $HN{=}C(CH_3)_2$ (red dashed line) as well as the trans- (blue dotted line) and cis- (blue dotted and dashed line) $CH_3N{=}CHCH_3$. The best fit to the data is obtained for a branching ratio trans-$CH_3N{=}CHCH_3$:cis-$CH_3N{=}CHCH_3$:$HN{=}C(CH_3)_2$ of 1:0.2:0.8.

4.4 CH + $(CH_3)_3N$

The 6 most likely exit channels for the CH reaction with TMA are formation of the fully methyl substituted imine and amino carbene, detected at m/z 71 (R4a, and b), as well as the dimethylimines (R4c, c' and d) and dimethyl amino carbenes (R4e and f) at m/z 57. The enthalpies in R4g and R4i are for the trans isomers. Formation of the methyl substituted imines or amino carbene, detected at m/z 43, by loss of a C_2H_5 radical are also exothermic.

$CH + (CH_3)_3N \rightarrow$	$CH_3N{=}C(CH_3)_2$	+ H	-339.62 kJ.mol^{-1}	R4a
	$(CH_3)_2N{-}CCH_3$	+ H	-158.76 kJ.mol^{-1}	R4b
	trans-$CH_3N{=}CHCH_3$	+ CH_3	-295.73 kJ.mol^{-1}	R4c
	cis-$CH_3N{=}CHCH_3$	+ CH_3	-279.73 kJ.mol^{-1}	R4c'
	$HN{=}C(CH_3)_2$	+ CH_3	-329.73 kJ.mol^{-1}	R4d
	trans-$CH_3HN{-}CCH_3$	+ CH_3	-152.25 kJ.mol^{-1}	R4e
	cis-$CH_3HN{-}CCH_3$	+ CH_3	-131.93 kJ.mol^{-1}	R4e'
	$(CH_3)_2N{-}CH$	+ CH_3	-113.11 kJ.mol^{-1}	R4f
	$HN{=}CHCH_3$	+ C_2H_5	-398.17 kJ.mol^{-1}	R4g
	$CH_3N{=}CH_2$	+ C_2H_5	- 362.35 kJ.mol^{-1}	R4h
	$CH_3HN{-}CH$	+ C_2H_5	- 213.99 kJ.mol^{-1}	R4i
	$H_2N{-}CCH_3$	+ C_2H_5	- 253.82 kJ.mol^{-1}	R4j

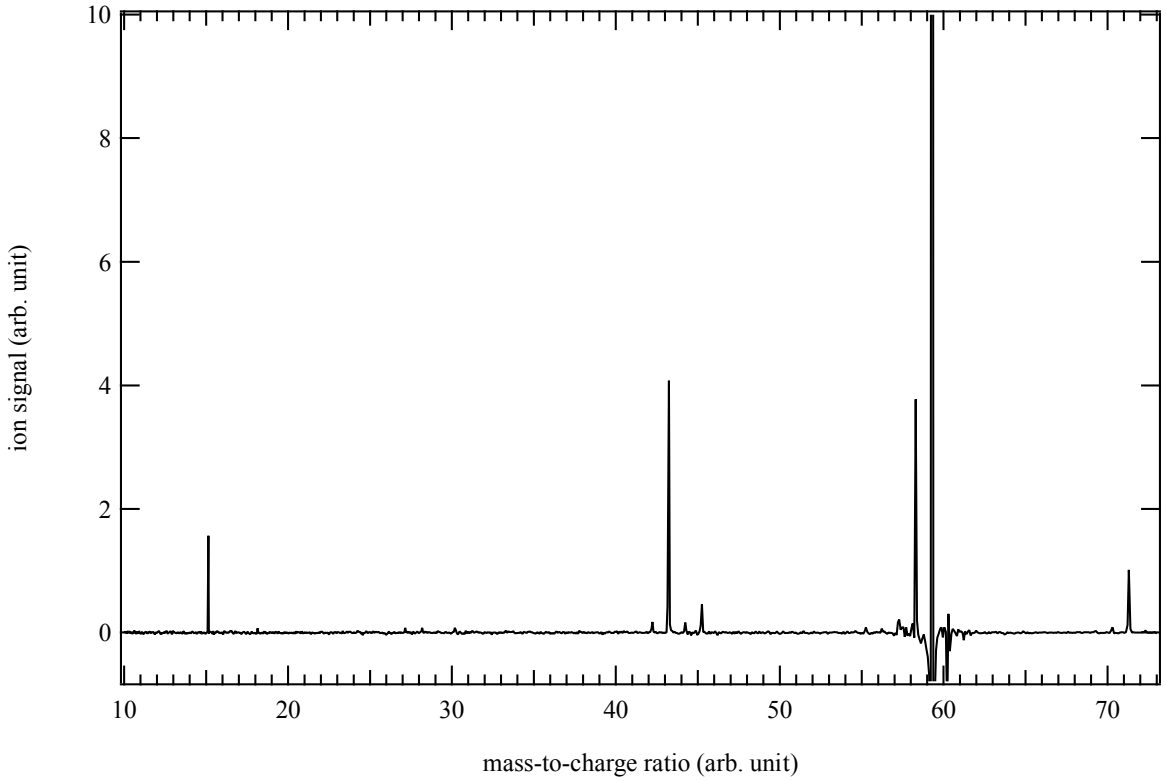

Figure 9. Mass spectrum obtained by photolysis of a $CHBr_3$ and $(CH_3)_3NH$ mixture in helium and nitrogen integrated over the 8.2–10.3 eV photon energy and the 0–5 ms time range.

Figure 9 displays the mass spectrum obtained by photolysis of a $CHBr_3$ and $(CH_3)_3N$ mixture integrated over the 8.2–10.3 eV photon energy and the 0-5 ms time range. The main signals are detected at m/z 15, 43, 58, 59, and 71. Signal at m/z 59 is likely to come from the incomplete baseline subtraction of the large TMA signal. As for the reaction with DMA, signal at m/z 15 is identified as coming from ionization of the methyl radical formed in the reaction flow. Although not as prominent as for reaction R3, signal at m/z 42 is identified as propene (~9.7 eV). Signal at m/z 58 displays a fast kinetics and a photoionization spectrum with a lower ionization energy onset (~8.9 eV) than that discussed in Section 4.3 for the bromofrom/DMA mixture at the same m/z value. After a fast rise, the signal is found to decay rapidly, within 4 ms after the laser pulse, which is not consistent with the formation of a closed shell molecule

from the CH + TMA reaction. In this case the signal observed at m/z 58 could come from the dissociative ionization of a higher-mass radical species or direct photodissociation of TMA.

The photoionization spectrum recorded at m/z 43 for TMA and bromoform is similar to those recorded at the same m/z for DMA and bromoform and suggests the formation of $CH_3N{=}CH_2$. No signal is detected at m/z 29 for the expected C_2H_5 coproduct. In the case of the bromoform/TMA mixture, there is a very small signal at m/z 57 (Figure 9), representing less than 10% of the sum of all the signals at m/z 43, 57 and 71. Its photoionization spectrum is similar to that displayed in in Figure 8 (open circles). The good match between the two experimental photoion spectra confirms formation of the dimethylimine isomers in the flow, although with a much lower fraction than for the CH + DMA reaction.

Figure 10 displays photoionization spectrum of m/z 71 (open circles) recorded under the same experimental conditions as Figures 9. A large signal offset is observed below 8.5 eV. As for the reaction with MA and DMA, the temporal profile of the ions detected at low energy is constant after their formation upon irradiation by the laser pulse. In the case of reaction with TMA, signals are detected at m/z 150/152 as well as 151/153 possibly corresponding to the CHBr/CBr reaction adducts or products. Dissociative ionization of these larger mass molecule may contribute to the observed large signal. The lack of time dependence of the low energy m/z 71 suggests that the reactive trimethyl amino carbene isomers are not contributing significantly to the CH + TMA reaction products. Including a constant offset, the photoionization spectrum in Figure 10 is consistent with the formation of the $CH_3N{=}C(CH_3)_2$ isomer.

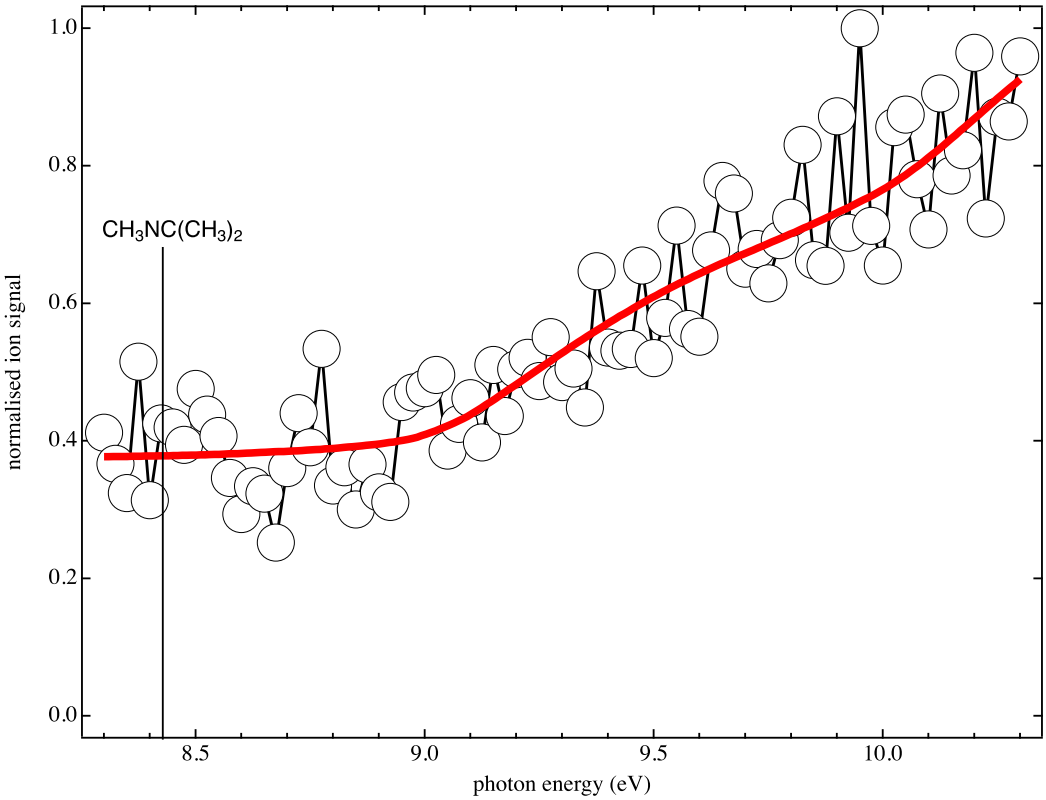

Figure 10. Photoionization spectrum of m/z 71 (open circles) obtained by photolysis of a $CHBr_3$ and $(CH_3)_3NH$ mixture in helium and nitrogen integrated over the 0−40 ms time range. The red solid line is the integrated photoelectron spectra $CH_3N{=}C(CH_3)_2$ (red dotted line) from Bock *et al.*[63].

5. DISCUSSION

5.1 Reaction mechanisms

The reaction of the CH radical with NH_3 has been studied both experimentally and theoretically.[15] The MCSCF/CASSCF PES reveals that the initial H_3N–CH complex is formed by a Lewis acid/base-type reaction for which the nitrogen donates electrons to the CH Lewis acid. This donor–acceptor interaction results in positive and negative charges on the nitrogen and carbon atoms, respectively. A similar mechanism has been proposed for reactions of singlet carbene compounds (CH_2, CHCl, CHF) with amines.[67] According to the CH + NH_3 PES,[15] the dative H_3N–CH complex is formed with no energy barrier leading to kinetics mainly controlled by long-range interactions. Scheme 1 displays the mechanism proposed by Blitz et al.[15] The

initial H_3N–CH adduct may directly dissociate to H_2N–CH + H or isomerize through H-atom transfer to form a more stable H_2N–CH_2 reaction intermediate. The most likely fate of the H_2N–CH_2 intermediate is dissociation to HN=CH_2 + H, either directly or through a second H-atom transfer followed by H-atom loss. The detection of only HN=CH_2 isomer as a product of the CH + NH_3 reaction in the present study agrees with the RRKM–ME branching ratios calculated on the PES by Blitz et al.[15] in which the H-loss from the initial H_3N–CH complex is predicted not to be a competitive channel.

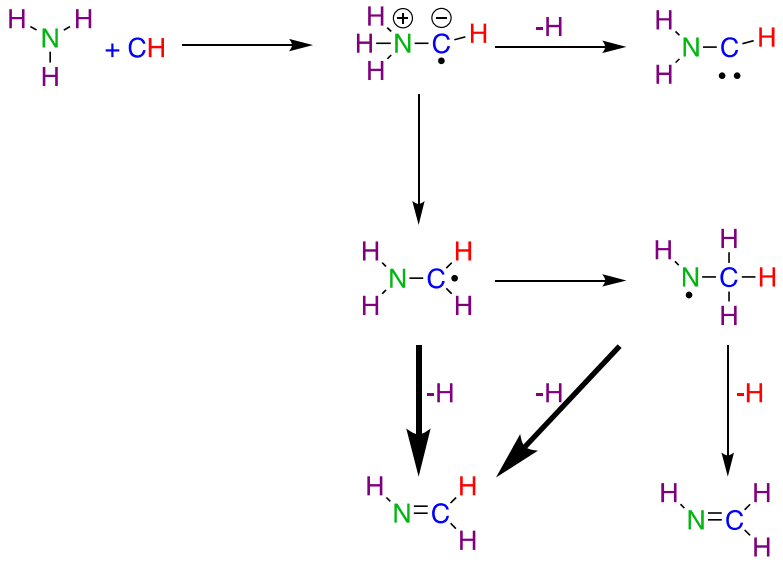

Scheme 1

The only channel leading to the imine HN=CH_2 through elimination of the hydrogen atom initially on the carbon atom involves two successive H-transfers from the nitrogen atom to the carbon atom to form the HN–CH_3 intermediate. In the case of the CD + NH_3 reaction, assuming that the deuteration has no effect on the unimolecular dissociation rate, dissociation of the HN–CH_2D intermediate would lead to a 2:1 ratio for HN=CHD:HN=CH_2. The detection of mainly m/z 30 from the CD + NH_3 reaction suggests that the second H transfer does not compete with the direct dissociation of the H_2N–CHD intermediate. The good agreement between the present work and the RRKM–ME performed on the high-level PES supports the dative-bond mechanism proposed by Blitz et al. for the CH + NH_3 reaction.

Although there is no theoretical information about the CH + NH_2CH_3 PES, Zabarnick *et al.*[14] suggest that the reaction proceeds through insertion of the CH radical into N–H or C–H bonds followed by a rapid decomposition of the reaction intermediates. Zabarnick et al. proposed these mechanisms based on the comparison of the measured reaction rate coefficients with those of the CH + NH_3 and CH + C_2H_6 reactions. In view of the PES calculated for the CH + NH_3,[15] as well as the proposed mechanism for CH_2, CHF, and CHCl singlet carbene with MA,[67] it is likely that the reaction may also proceed through the formation of a dative intermediate. Direct insertion into a C–H bond of the methyl group is likely to be a minor entrance channel as observed for unsaturated hydrocarbons.[40]

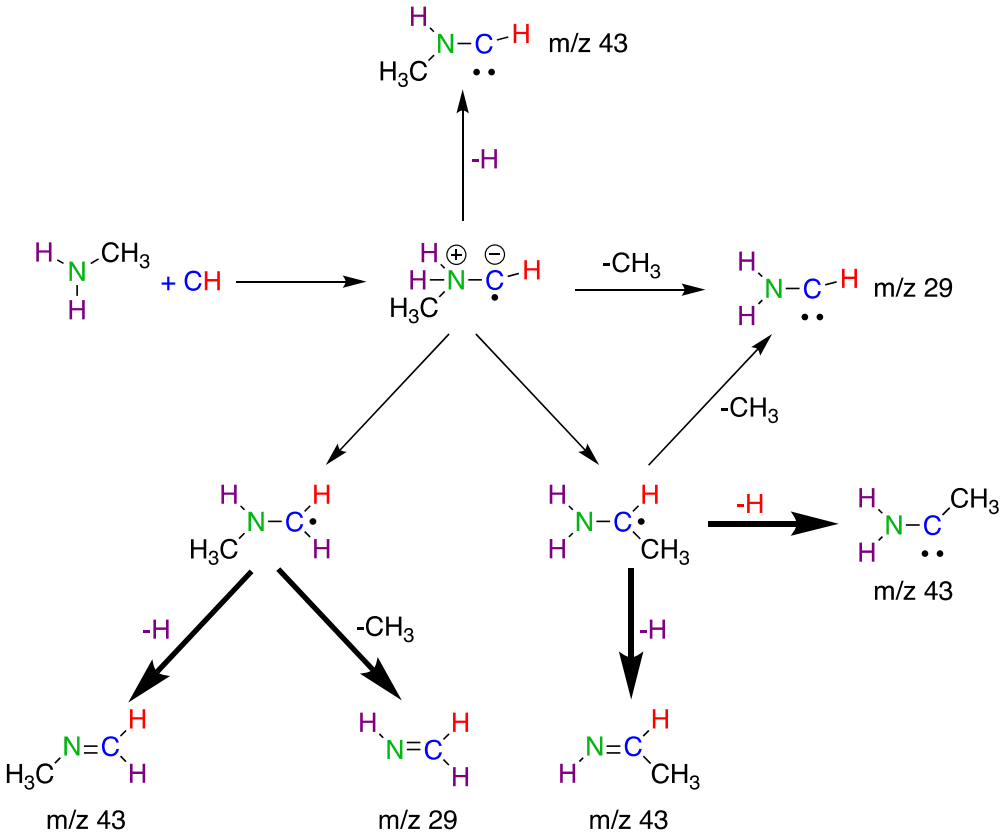

Scheme 2

Scheme 2 displays a proposed mechanism for the CH + CH_3NH_2 reaction starting from the formation of the dative CH_3H_2N–CH intermediate. Bold arrows correspond to observed channels. The detection of m/z 15, 29, and 43 supports the fact that the reaction proceeds

through both H- and CH_3-loss. We have no evidence to support direct dissociation of the CH_3NH_2–CH dative adduct by H-loss to form the CH_3HN–CH methyl amino carbene at m/z 43 or CH_3–loss to form the H_2N–CH isomer at m/z 29. The dative intermediate is therefore more likely to isomerize through either H- or CH_3-transfer to give CH_3HN–CH_2 and/or H_2N–$CHCH_3$ intermediates. The so-formed CH_3HN–CH_2 isomer can lose either a H atom or a CH_3 group to give the detected $CH_3N=CH_2$ and $HN=CH_2$ final imine products. The H_2N–$CHCH_3$ intermediate resulting from the CH_3 transfer can lose one of the two H-atoms on the nitrogen to form the cis or trans $HN=CHCH_3$ imines or the H-atom initially on the carbon atom of the CH radical to form the H_2N–CCH_3 amino carbene. Loss of the methyl group on the carbon atom leads to the H_2N–CH amino carbene. We have no evidence of the H_2N–CH and H_2N–$CHCH_3$ amino carbene in the reaction flow.

The 0.9:1 branching ratio for $CH_3N=CH_2$:$HN=CHCH_3$ at m/z 43 (Figure 5) suggests that the CH_3-tranfer may compete with the H-transfer following the formation of the initial dative adduct. In recent literature, methyl-group transfers have not been necessary to explain the observed reaction products from a CH reaction with saturated or unsaturated hydrocarbons.[40] In order to gain additional knowledge about the likelihood of the methyl-group transfer, the saddle points for the H- and CH_3-transfers from the CH_3H_2N–CH intermediate have been calculated at the CBS–QB3 level of theory. Figure 11 displays the energetics for the initial reaction adduct, the two isomers resulting from the H- and CH_3-transfer, as well as the corresponding saddle points. All the energies are calculated relatively to that of the reactants. At this level of theory the saddle point for the H-transfer is found to be below that of the reactants while that for the CH_3-tranfer is 17.1 $kJ.mol^{-1}$ above that of CH + CH_3NH_2.

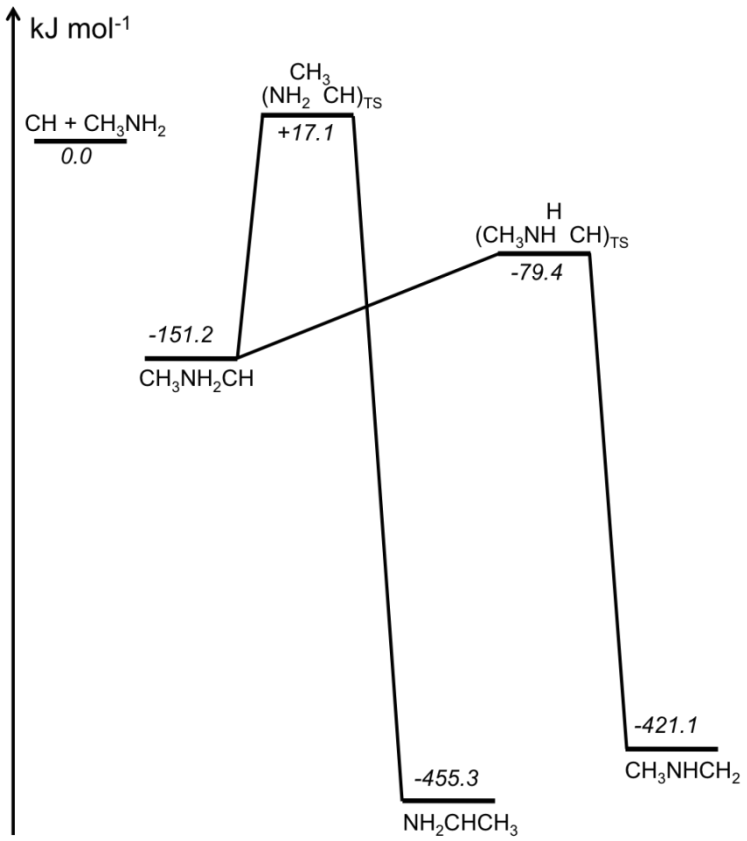

Figure 11. C_2H_6N stationary points calculated using the CBS–QB3 method.

Estimates for absolute uncertainty of the CBS–QB3 method[68] make it unlikely that the CBS–QB3 saddle point energy for methyl transfer lies below the reactant energy. Although the CBS–QB3 method has been shown not to be appropriate to calculate the energy of a dative interaction,[68,69] the relative energies of the two saddle points displayed in Figure 11 show that the CH_3 transfer is energetically less favorable than the H-transfer. As suggested for B–N dative bonds, the MP2 method and higher level methods may be more appropriate for such studies.[69] The detection of $HN{=}CHCH_3$ from the CH + CH_3NH_2 reaction may be explained by a lowering of the CH_3-transfer transition state below that of the reactants due to the dative interaction. Alternatively, direct insertion of the CH radical into the N–C or a methyl C–H bond could become a competitive entrance channel. Scheme 3 displays a possible mechanism for radical insertion into a C–H bond requiring only one H-atom transfer (and no CH_3 transfer) to form the H_2N–$CHCH_3$ intermediate. Loss of a H-atom from the nitrogen forms the cis- or trans-

methylimine isomers. It is possible that such a mechanism become more favorable as the number of methyl groups on the reactant amine increases. Further calculations at a higher level of theory are required in order to discriminate between the direct insertion and dative intermediate mechanisms for this reaction.

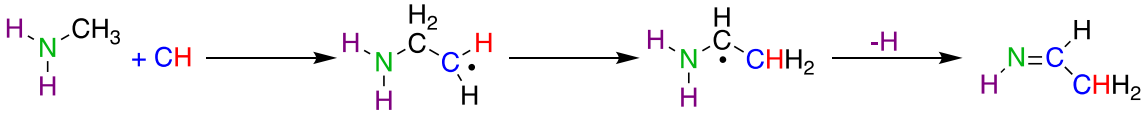

Scheme 3

The CH + $(CH_3)_2NH$ reaction may be discussed using a similar dative mechanism as those described for the CH + NH_3 and CH + CH_3NH_2 reactions. As for the reaction of CH with MA, the product detection study does not allow differentiating between a direct N–H/N–C insertion and an addition/isomerization entrance channel. The non-detection of the reactive $(CH_3)_2N$–CH and CH_3HN–CH amino carbenes suggests that direct decomposition of the $(CH_3)_2HN$–CH dative adduct through H- or CH_3-loss is not a competitive channel. Scheme 4 shows the proposed mechanism based on the isomerization of a datively bond intermediate to form imine products. Bold arrows correspond to observed channels. Pathways to amino carbene compounds are not shown.

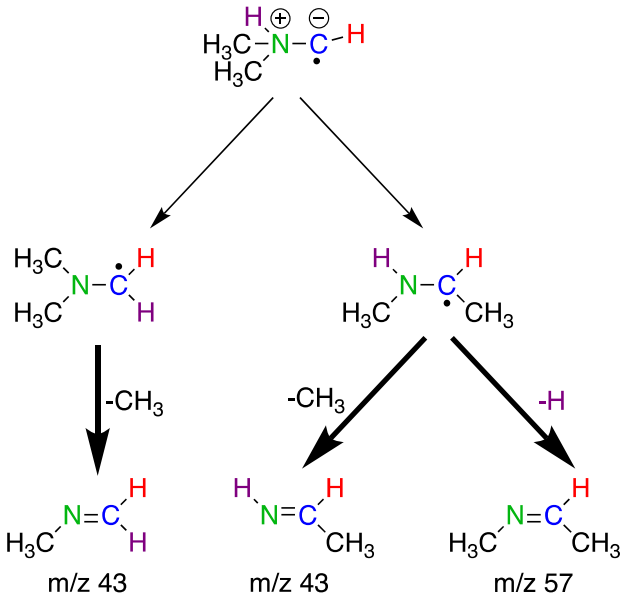

Scheme 4

The initial $(CH_3)_2HN–CH$ dative intermediate may isomerize to $(CH_3)_2N–CH_2$ or $CH_3HN–CHCH_3$ through H- or CH_3-transfers, respectively. The detection of $CH_3N=CH_2$ and $HN=CHCH_3$ may be explained by loss of a methyl group on the nitrogen atom from the H-transfer and the CH_3-transfer isomers. Loss of a H atom from the $CH_3HN–CHCH_3$ isomer leads to the observed $CH_3N=CHCH_3$ product at m/z 57. The $CH_3HN–CHCH_3$ intermediate may also be formed through a more direct C–H insertion mechanism as proposed in scheme 3 for the methyl substituted amine. The fit to the photoionization spectrum in Figure 8 suggests the detection of the $HN=C(CH_3)_2$ isomer. Its formation through the formation of the dative intermediate would require the transfer of two methyl groups from the nitrogen atom to the carbon atom to give the $HN–CH(CH_3)_2$ intermediate or one methyl group through a C–H or N–C insertion mechanism.

The main observed H- and CH_3-loss products from the CH + $(CH_3)_3N$ reaction are $CH_3N=CH_2$ and $HN=CHCH_3$ at m/z 43 and $CH_3N=C(CH_3)_2$ at m/z 71. Isomers at m/z 57 are also detected but are a minor pathway with an overall ion signal representing only 10% of the identified reaction products. Scheme 5 displays the possible reaction pathways following isomerization of the $(CH_3)_3N–CH$ dative adduct by methyl transfer or isomerization of the C–H insertion adduct by H-transfer. Bold arrows correspond to observed channels. The minor dimethylimine channel detected at m/z 57 may be formed by methyl loss from the $(CH_3)_2N–CHCH_3$ intermediate to give $CH_3N–CHCH_3$. Formation of $HN=C(CH_3)_2$ would require a methyl group transfer and a H-transfer, which is unlikely.

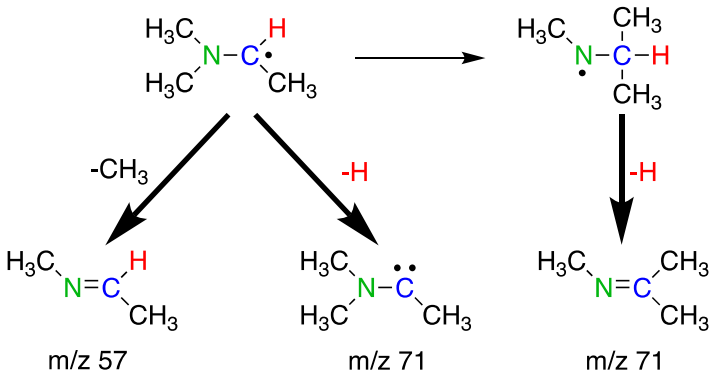

Scheme 5

In scheme 5, formation of the $CH_3N{=}C(CH_3)_2$ isomer at m/z 71 requires the transfer of a CH_3 group from the $(CH_3)_2N{-}CHCH_3$ intermediate to form a $CH_3N{-}CH(CH_3)_2$ intermediate followed by H-loss. This mechanism is similar to the successive two-H-atom transfers predicted by Blitz *et al.*[15] for the CH + NH_3 reaction. High-level quantum calculations and RRKM-based master equation calculations would be useful to explore these mechanisms in more detail. Formation of methylimine products by the CH + TMA reaction requires the loss of an ethyl group. Although we do detect methylimines at m/z = 43 in this reaction, the absence of signal from the expected co-product C_2H_5 radical (IE=8.12 eV)[65] in Figure 9 is puzzling.

5.2 Relevance for combustion chemistry

Prediction of NOx formation from combustion processes is a very active subject of research, especially due to the increasing use of fuels derived from biogenic sources (*e.g.,* biomass, agricultural wastes).[70-74] Biomass combustion could contribute to nitrogen conversion through the formation of nitrogenized intermediates such as HCN. Their formation may depend on the fuel structure. Accordingly, several studies have focused on flames burning nitrogenized compounds (*e.g.,* ammonia, pyrrole, pyridine).[75-80] The spatial detection of nitrogen containing radicals in laminar flames of DMA, ethylamine,[81] and morpholine[82] suggests that the NH_2 radical is formed very early in the combustion process and further reacts to form HCN, CN, and NO. The mole fraction of ammonia is also found to be relatively large ($6{\times}10^{-2}$) and is likely

to play a role in the formation of nitrogen reactive species and nitrogen containing hydrocarbons. The reactions of ammonia with other abundant combustion radicals is therefore likely to affect the formation of NH_2 radicals and ultimately NO. In the present study, the abstraction channel $NH_2 + CH_2$ from the $CH + NH_3$ reaction is not detected at the temperature of the flow (373 K). This product channel is calculated to be endothermic by 20.9 kJ mol^{-1} (CCSD(T))[15] and could become accessible at flame temperatures (>2000 K). The formation of the thermodynamically favorable $HN=CH_2$ may still remain a dominant pathway. Further reaction of the detected imine may lead to larger nitrogen containing molecules and contribute to incorporating nitrogen in large hydrocarbons such as polycyclic nitrogen containing aromatic hydrocarbons.

Imine and methyl substituted imines have been detected during the combustion of biomass model fuels.[82] As for ammonia, the reaction of methyl substituted amines with the CH radical may contribute to their formation and to the overall molecular growth scheme in combustion. Abstraction of a H-atom from the carbon group substituent may become more likely as the number of C–H bonds increase. The product detection preformed in the present study together with the temperature independent rate coefficient reported by Zabarnick *et al.*[14] suggest that the addition–elimination mechanism will still play a role even at combustion-relevant temperatures. The isomer resolved detection of the methyl substituted imines and their proposed formation mechanisms is likely to improve the quality of the chemical models used to reproduce their spatial molar fraction in flames.[82]

VI. CONCLUSION

The systematic study of the reaction of the methylidyne radical with ammonia, methyl, dimethyl, and trimethyl amine provides empirical evidence supporting a general reaction mechanism for CH reacting with amines. The detection of mainly the imine isomer upon reaction of CH with ammonia is in agreement with the mechanism proposed by Blitz *et al.*[15]

based on high-level calculations and RRKM-based master equation calculations. According to this mechanism, the insertion of the CH radical onto a N–H bond proceeds by the initial formation of a dative C–N bond. The donor–acceptor type mechanism is barrierless and is likely to occur over a wide range of temperatures, including under combustion conditions.

Although no theoretical data are available for the CH reaction with methyl substituted amines, a similar mechanism as that proposed for the reaction with ammonia may be employed to interpret the products detected for the CH + MA, DMA, and TMA. For each reaction, the detection of H- and CH_3-loss products may be explained in part through isomerization of an initial dative adduct formed by the sharing of the nitrogen lone pair with the carbon atom of the CH radical. Kinetic traces of the reaction products show no evidence of the formation of the reactive methyl-substituted amino carbene isomers. The detection of the methylimine with the methyl group on the carbon atom in the case of the CH + MA reaction suggests that the transfer of a methyl group could be a competitive pathway, but our calculations show a barrier well above reactant energy for this process. However, a direct insertion pathway of the CH radical into a methyl C–H bond may become competitive as the number of methyl group increases. Our data do not allow differentiating between a dative mechanism and direct insertion, but provide evidence that the latter should be considered. In the case of the CH + TMA reaction, direct insertion of the CH radical into a C–H bond would lead to a pathway involving only one CH_3-transfer followed by H-loss to explain the formation of the detected $CH_3N{=}C(CH_3)_2$ isomer. Methylimine isomers are detected from both the CH + DMA and CH + TMA reactions. The lack of imine absolute ionization cross section does not allow to quantify their branching fractions. In the case of the CH + TMA reaction formation of methylimines should also produce a C_2H_5 radical, which we do not observe.

Overall the dative reaction mechanism proposed by Blitz *et al.*[15] for the CH + NH_3 reaction as well as Ramasami *et al.*[67] for the CH_2/CHCl/CHF + CH_3NH_2 is not sufficient to

explain all the detected products and a C–H insertion mechanism is likely to become favorable for alklyl substituted amines. Although the present studies provide valuable data for the understanding of the reactivity of amines with the CH radical, further theoretical studies including RRKM-based master equations on the potential energy surface and experimental studies of photoionization cross sections are paramount toward the full understanding of the reaction mechanism, especially about the competition between direct N–C insertion and formation of an initial dative intermediate.

ACKNOWLEDGEMENTS

The Rennes team acknowledges support from the Agence Nationale de la Recherche, contract ANR-11-BS04-024- CRESUSOL-01, the French INSU/CNRS Program ‘‘Physique et Chimie du Milieu Interstellaire’’ (PCMI), the Institut Nationalde Physique (INPCNRS), the Région Bretagne and the Université de Rennes 1. S.D.L.P. acknowledges financial support from the Institut Universitaire de France. FG and KLC acknowledge travel support from the Eberly College of Art and Sciences and The Bennett Department of Chemistry at West Virginia University as well as the WVU Research Corporation PSCoR program. We thank Messrs. Howard Johnsen and Raybel Almeida for technical support of this experiment. D.L.O. and the instrumentation for this work are supported by the Division of Chemical Sciences, Geosciences, and Biosciences, the Office of Basic Energy Sciences, the U.S. Department of Energy. Sandia National Laboratories is a multimission laboratory managed and operated by National Technology and Engineering Solutions of Sandia, LLC., a wholly owned subsidiary of Honeywell International, Inc. for the U.S. DOE’s National Nuclear Security Administration under contract DE-NA0003525. This paper describes objective technical results and analysis. Any subjective views or opinions that might be expressed in the paper do not necessarily represent the views of the USDOE or the United States Government. This research used resources of the Advanced Light Source, a DOE Office of Science User Facility, which is

supported by the Direct, Office of Science, Office of Basic Energy Sciences, the U.S. Department of Energy under contract DE-AC02-05CH11231 at Lawrence Berkeley National Laboratory.

Supporting Information: Normalized integrated Franck-Condon factors and photoelectron spectra of the imines and amino carbene isomers.

References

(1) Ge, X.; Wexler, A. S.; Clegg, S. L. Atmospheric amines–Part II. Thermodynamic properties and gas/particle partitioning. *Atmos. Environ.* **2011**, *45*, 561-577.

(2) Ge, X.; Wexler, A. S.; Clegg, S. L. Atmospheric amines–Part I. A review. *Atmos. Environ.* **2011**, *45*, 524-546.

(3) Cullis, C. F.; Khokhar, B. A. The inhibiting influence of aliphatic amines on the explosive oxidation of acethayldehyde. *Trans. Faraday Society* **1960**, *56*, 1235-1244.

(4) Shi, J. C.; Shang, Y. L.; Ye, W.; Zhang, R. T.; Luo, S. N. Shock-tube experiments and chemical kinetic modeling study of CH_4 sensitized by CH_3NHCH_3. *Energy & Fuels* **2018**, *32*, 5588-5595.

(5) Moore, F.; Tipper, C. F. H. The effect of additives on low-temperature hydrocarbon ignition in a flow system. *Combust. Flame* **1972**, *19*, 81-87.

(6) Lucassen, A.; Zhang, K.; Warkentin, J.; Moshammer, K.; Glarborg, P.; Marshall, P.; Kohse-Höinghaus, K. Fuel-nitrogen conversion in the combustion of small amines using dimethylamine and ethylamine as biomass-related model fuels. *Combust. Flame* **2012**, *159*, 2254-2279.

(7) Tipper, C. F. H.; Titchard, A. The effect of additives on the cool flame combustion of n-heptane. *Combust. Flame* **1971**, *16*, 223-232.

(8) Jones, P. W.; Selby, K.; Tidball, M. J.; Waddington, D. J. Inhibition of gas-phase oxidation reactions by aliphatic amines and related compounds. *Combust. Flame* **1974**, *22*, 209-217.

(9) Atkinson, R.; Pitts Jr, J. N. Kinetics of the reactions of O (^{3}P) atoms with the amines CH_3NH_2, $C_2H_5NH_2$,$(CH_3)_2NH$, and $(CH_3)_3N$ over the temperature range 298–440 K. *J. Chem. Phys.* **1978**, *68*, 911-915.

(10) Slagle, I. R.; Dudich, J. F.; Gutman, D. Direct identification of reactive routes in the reaction of oxygen atoms with dimethylamine. *Chem. Phys. Lett.* **1979**, *61*, 620-624.

(11) Atkinson, R.; Baulch, D. L.; Cox, R. A.; Crowley, J. N.; Hampson, R. F.; Hynes, R. G.; Jenkin, M. E.; Rossi, M. J.; Troe, J. Evaluated kinetic and photochemical data for atmospheric chemistry: Volume I - gas phase reactions of O_x, HO_x, NO_x and SO_x species. *Atmos. Chem. Phys.* **2004**, *4*, 1461-1738.

(12) Sims, I. R.; Queffelec, J. L.; Defrance, A.; Rebrionrowe, C.; Travers, D.; Bocherel, P.; Rowe, B. R.; Smith, I. W. M. Ultralow temperature kinetics of neutral-neutral reactions - The technique and results for the reactions CN + O_2 down to 13 K and CN+NH_3 down to 25 K. *J. Chem. Phys.* **1994**, *100*, 4229-4241.

(13) Nizamov, B.; Leone, S. R. Rate Coefficients and Kinetic Isotope Effect for the C_2H Reactions with NH_3 and ND_3 in the 104− 294 K Temperature Range. *J. Phys. Chem. A* **2004**, *108*, 3766-3771.

(14) Zabarnick, S.; Fleming, J. W.; Lin, M. C. Kinetics of the methylidyne (CHX^2PI) radical reactions with ammonia and methylamines. *Chem. Phys.* **1989**, *132*, 407-411.

(15) Blitz, M. A.; Talbi, D.; Seakins, P. W.; Smith, I. W. M. Rate constants and branching ratios for the reaction of CH radicals with NH_3: A combined experimental and theoretical study. *J. Phys. Chem. A* **2012**, *116*, 5877-5885.

(16) Corchado, J. C.; Espinosa-Garcia, J.; Hu, W.-P.; Rossi, I.; Truhlar, D. G. Dual-level reaction-path dynamics (the approach to VTST with semiclassical tunneling). Application to OH+ NH_3. fwdarw. H_2O+ NH_2. *J. Phys. Chem.* **1995**, *99*, 687-694.

(17) Meads, R. F.; Maclagan, R. G.; Phillips, L. F. Kinetics, energetics, and dynamics of the reactions of cyanogen with ammonia and ammonia-d3. *J. Phys. Chem.* **1993**, *97*, 3257-3265.

(18) Tian, W.; Wang, W.; Zhang, Y.; Wang, W. Direct dynamics study on the mechanism and the kinetics of the reaction of CH_3NH_2 with OH. *Int. J. Quantum Chem* **2009**, *109*, 1566-1575.

(19) Onel, L.; Blitz, M. A.; Breen, J.; Rickardcd, A. R.; Seakins, P. W. Branching ratios for the reactions of OH with ethanol amines used in carbon capture and the potential impact on carcinogen formation in the emission plume from a carbon capture plant. *Phys. Chem. Chem. Phys.* **2015**, *17*, 25342-25353.

(20) Onel, L.; Blitz, M.; Dryden, M.; Thonger, L.; Seakins, P. Branching ratios in reactions of OH radicals with methylamine, dimethylamine, and ethylamine. *Environ. Sci. Technol.* **2014**, *48*, 9935-9942.

(21) Onel, L.; Thonger, L.; Blitz, M. A.; Seakins, P. W.; Bunkan, A. J. C.; Solimannejad, M.; Nielsen, C. J. Gas-phase reactions of OH with methyl amines in the presence or absence of molecular oxygen. An experimental and theoretical study. *J. Phys. Chem. A* **2013**, *117*, 10736-10745.

(22) Onel, L.; Blitz, M. A.; Seakins, P. W. Direct determination of the rate coefficient for the reaction of OH radicals with monoethanol amine (MEA) from 296 to 510 K. *J. Phys. Chem. Lett.* **2012**, *3*, 853-856.

(23) Love, N.; Parthasarathy, R. N.; Gollahalli, S. R. Concentration measurements of CH and OH radicals in laminar biofuel flames. *Int. J. Green Energy* **2011**, *8*, 113-120.

(24) Tinaut, F. V.; Reyes, M.; Giménez, B.; Pastor, J. V. Measurements of OH* and CH* chemiluminescence in premixed flames in a constant volume combustion bomb under autoignition conditions. *Energy & Fuels* **2010**, *25*, 119-129.

(25) Glarborg, P.; Miller, J. A.; Ruscic, B.; Klippenstein, S. J. Modeling nitrogen chemistry in combustion. *Prog. Energy Combust. Sci.* **2018**, *67*, 31-68.

(26) Vereecken, L.; Pierloot, K.; Peeters, J. B3LYP-DFT characterization of the potential energy surface of the CH ($X^2\Pi$)+ C_2H_2 reaction. *J. Chem. Phys.* **1998**, *108*, 1068-1080.

(27) Vereecken, L.; Peeters, J. Detailed microvariational RRKM master equation analysis of the product distribution of the C_2H_2+ CH ($X^2\Pi$) reaction over extended temperature and pressure ranges. *J. Phys. Chem. A* **1999**, *103*, 5523-5533.

(28) Goulay, F.; Trevitt, A. J.; Meloni, G.; Selby, T. M.; Osborn, D. L.; Taatjes, C. A.; Vereecken, L.; Leone, S. R. Cyclic versus linear isomers produced by reaction of the methylidyne radical (CH) with small unsaturated hydrocarbons. *J. Am. Chem. Soc.* **2009**, *131*, 993-1005.

(29) Fenimore, C. P. Formation of nitric oxide in premixed hydrocarbon flames. *Proc. Comb. Instit.* **1971**, *13*, 373–380.

(30) Miller, J. A.; Bowman, C. T. Mechanism and modeling of nitrogen chemistry in combustion. *Prog. Energy Combust. Sci.* **1989**, *15*, 287-338.

(31) Becker, K. H.; Engelhardt, B.; Geiger, H.; Kurtenbach, R.; Schrey, G.; Wiesen, P. Temperature dependence of the CH+ N_2 reaction at low total pressure. *Chem. Phys. Lett.* **1992**, *195*, 322-328.

(32) Becker, K. H.; Engelhardt, B.; Geiger, H.; Kurtenbach, R.; Weisen, P. Temperature dependence of the reactions of CH radicals with NO, NH_3 and N_2O in the range 200–1300 K. *Chem. Phys. Lett.* **1993**, *210*, 135-140.

(33) Becker, K. H.; Engelhardt, B.; Geiger, H.; Kurtenbach, R.; Wiesen, P. Temperature dependence of the reactions of CH radicals with NO, NH_3 and N_2O in the range 200-1300-K. *Chem. Phys. Lett.* **1993**, *210*, 135-140.

(34) Geiger, H.; Wiesen, P.; Becker, K. H. A product study of the reaction of CH radicals with nitric oxide at 298 K. *Phys. Chem. Chem. Phys.* **1999**, *1*, 5601-5606.

(35) Cui, Q.; Morokuma, K.; Bowman, J. M.; Klippenstein, S. J. The spin-forbidden reaction CH ($^2\Pi$)+ N_2→ HCN+ N (^4S) revisited. II. Nonadiabatic transition state theory and application. *J. Chem. Phys.* **1999**, *110*, 9469-9482.

(36) Moskaleva, L. V.; Lin, M. C. The spin-conserved reaction CH+ N_2→ H+ NCN: A major pathway to prompt NO studied by quantum/statistical theory calculations and kinetic modeling of rate constant. *Proc. Comb. Instit.* **2000**, *28*, 2393-2401.

(37) Berman, M. R.; Tsuchiya, T.; Gregušová, A.; Perera, S. A.; Bartlett, R. J. HNNC radical and its role in the CH+ N2 reaction. *J. Phys. Chem. A* **2007**, *111*, 6894-6899.

(38) Goos, E.; Sickfeld, C.; Mauß, F.; Seidel, L.; Ruscic, B.; Burcat, A.; Zeuch, T. Prompt NO formation in flames: The influence of NCN thermochemistry. *Proc. Comb. Instit.* **2013**, *34*, 657-666.

(39) Bocherel, P.; Herbert, L. B.; Rowe, B. R.; Sims, I. R.; Smith, I. W.; Travers, D. Ultralow-temperature kinetics of CH ($X^2\Pi$) reactions: Rate coefficients for reactions with O_2 and NO (T= 13− 708 K), and with NH_3 (T= 23− 295 K). *J. Phys. Chem.* **1996**, *100*, 3063-3069.

(40) Trevitt, A. J.; Goulay, F. Insights into gas-phase reaction mechanisms of small carbon radicals using isomer-resolved product detection. *Phys. Chem. Chem. Phys.* **2016**, *18*, 5867-5882.

(41) Osborn, D. L.; Zou, P.; Johnsen, H.; Hayden, C. C.; Taatjes, C. A.; Knyazev, V. D.; North, S. W.; Peterka, D. S.; Ahmed, M.; Leone, S. R. The multiplexed chemical kinetic photoionization mass spectrometer: A new approach to isomer-resolved chemical kinetics. *Rev. Sci. Instrum.* **2008**, *79*, 104103: 1-10.

(42) Taatjes, C. A.; Hansen, N.; Osborn, D. L.; Kohse-Höinghaus, K.; Cool, T. A.; Westmoreland, P. R. "Imaging" combustion chemistry via multiplexed synchrotron-photoionization mass spectrometry. *Phys. Chem. Chem. Phys.* **2008**, *10*, 20-34.

(43) Goulay, F.; Trevitt, A. J.; Savee, J. D.; Bouwman, J.; Osborn, D. L.; Taatjes, C. A.; Wilson, K. R.; Leone, S. R. Product detection of the CH radical reaction with acetaldehyde. *J. Phys. Chem. A* **2012**, *116*, 6091-6106.

(44) Zou, P.; Shu, J.; Sears, T. J.; Hall, G. E.; North, S. W. Photodissociation of bromoform at 248 nm: Single and multiphoton processes. *J. Phys. Chem. A* **2004**, *108*, 1482-1488.

(45) Romanzin, C.; Boye-Peronne, S.; Gauyacq, D.; Benilan, Y.; Gazeau, M. C.; Douin, S. CH radical production from 248 nm photolysis or discharge-jet dissociation of CHBr3 probed by cavity ring-down absorption spectroscopy. *J. Chem. Phys.* **2006**, *125*, 114312: 1-9.

(46) Bourgalais, J.; Spencer, M.; Osborn, D. L.; Goulay, F.; Le Picard, S. D. Reactions of atomic carbon with butene isomers: Implications for molecular growth in carbon-rich environments. *J. Phys. Chem. A* **2016**, *120*, 9138-9150.

(47) Capron, M.; Bourgalais, J.; Kailasanathan, R. K. A.; Osborn, D. L.; Le Picard, S. D.; Goulay, F. Flow tube studies of the C (^{3}P) reactions with ethylene and propylene. *Phys. Chem. Chem. Phys.* **2015**, *17*, 23833-23846.

(48) Montgomery, J. A.; Frisch, M. J.; Ochterski, J. W.; Petersson, G. A. A complete basis set model chemistry. VI. Use of density functional geometries and frequencies. *J. Chem. Phys.* **1999**, *110*, 2822-2827.

(49) Montgomery, J. A.; Frisch, M. J.; Ochterski, J. W.; Petersson, G. A. A complete basis set model chemistry. VII. Use of the minimum population localization method. *J. Chem. Phys.* **2000**, *112*, 6532-6542.

(50) Barone, V.; Bloino, J.; Biczysko, M.; Santoro, F. Fully integrated approach to compute vibrationally resolved optical spectra: from small molecules to macrosystems. *J. Chem. Theo. Comput.* **2009**, *5*, 540-554.

(51) Goulay, F.; Rebrion-Rowe, C.; Biennier, L.; Le Picard, S. D.; Canosa, A.; Rowe, B. R. Reaction of anthracene with CH radicals: An experimental study of the kinetics between 58 and 470 K. *J. Phys. Chem. A* **2006**, *110*, 3132-3137.

(52) Herbert, L. B.; Sims, I. R.; Smith, I. W. M.; Stewart, D. W. A.; Symonds, A.; Canosa, A.; Rowe, B. R. Rate constants for the relaxation of CH(X(2)pi,nu=1) by CO and N-2 at temperatures from 23 to 584 K. *J. Phys. Chem.* **1996**, *100*, 14928-14935.

(53) Brownsword, R. A.; Herbert, L. B.; Smith, I. W. M.; Stewart, D. W. A. Pressure and temperature dependence of the rate constants for the association reactions of CH radicals with CO and N-2 between 202 and 584 K. *J. Chem. Soc., Faraday* **1996**, *92*, 1087-1094.

(54) Ruzsicska, B. P.; Jodhan, A.; Choi, H. K. J.; Strausz, O. P.; Bell, T. N. Chemistry of carbynes: reaction of CF, CCl, and CBr with alkenes. *J. Am. Chem. Soc.* **1983**, *105*, 2489-2490.

(55) James, F. C.; Ruzsicska, B.; McDaniel, R. S.; Dickson, R.; Strausz, O. P.; Bell, T. N. Rate constants for the reaction of the bromomethyne radical with alkynes. *Chem. Phys. Lett.* **1977**, *45*, 449-453.

(56) McDaniel, R. S.; Dickson, R.; James, F. C.; Strausz, O. P.; Bell, T. N. Rate parameters for the reactions of the bromomethyne radical. *Chem. Phys. Lett.* **1976**, *43*, 130-134.

(57) Daugey, N.; Caubet, P.; Retail, B.; Costes, M.; Bergeat, A.; Dorthe, G. Kinetic measurements on methylidyne radical reactions with several hydrocarbons at low temperatures. *Phys. Chem. Chem. Phys.* **2005**, *7*, 2921-2927.

(58) Canosa, A.; Sims, I. R.; Travers, D.; Smith, I. W. M.; Rowe, B. R. Reactions of the methylidine radical with CH_4, C_2H_2, C_2H_4, C_2H_6, and but-1-ene studied between 23 and 295K with a CRESU apparatus. *Astron. Astrophys.* **1997**, *323*, 644-651.

(59) Goulay, F.; Derakhshan, A.; Maher, E.; Trevitt, A. J.; Savee, J. D.; Scheer, A. M.; Osborn, D. L.; Taatjes, C. A. Formation of dimethylketene and methacrolein by reaction of the CH radical with acetone. *Phys. Chem. Chem. Phys.* **2013**, *15*, 4049-58.

(60) Cheng, B.-M.; Lu, H.-C.; Chen, H.-K.; Bahou, M.; Lee, Y.-P.; Mebel, A. M.; Lee, L. C.; Liang, M.-C.; Yung, Y. L. Absorption cross sections of NH_3, NH_2D, NHD_2, and ND_3 in the spectral range 140-220 nm and implications for planetary isotopic fractionation. *Astrophys. J.* **2006**, *647*, 1535-1542.

(61) Hubin-Franskin, M.-J.; Delwiche, J.; Giuliani, A.; Ska, M.-P.; Motte-Tollet, F.; Walker, I. C.; Mason, N. J.; Gingell, J. M.; Jones, N. C. Electronic excitation and optical cross sections of methylamine and ethylamine in the UV–VUV spectral region. *J. Chem. Phys.* **2002**, *116*, 9261-9268.

(62) Halpern, A. M.; Ondrechen, M. J.; Ziegler, L. D. Analysis of the absoprtion and fluorescence spectra of trimethylamine - Determination of the A-X origin and the ground-state inversion barrier. *J. Am. Chem. Soc.* **1986**, *108*, 3907-3912.

(63) Bock, H.; Dammel, R. Methanimines RR'C=NR" - Preparation and photoelectron spectra. *Chemische Berichte-Recueil* **1987**, *120*, 1961-1970.

(64) Bobeldijk, M.; van der Zande, W. J.; Kistemaker, P. G. Simple models for the calculation of photoionization and electron impact ionization cross section of polyatomic molecules. *Chem. Phys.* **1994**, *179*, 125-130.

(65) NIST, 2005, Standard Reference Database Number 69, NIST Chemistry WebBook, National Institute of Standards and Technology, Gaithersburg MD, 20899 (http://webbook.nist.gov).

(66) Savee, J. D.; Welz, O.; Taatjes, C. A.; Osborn, D. L. New mechanistic insights to the O(^{3}P) + propene reaction from multiplexed photoionization mass spectrometry. *Phys. Chem. Chem. Phys.* **2012**, *14*, 10410-10423.

(67) Ramasami, K.; Ramalingam, M.; Venuvanalingam, P. Singlet methylene and halocarbenes insertions into polar N-H bonds of amines *J. Theo. Comput. Chem.* **2009**, *8*, 1143-1153.

(68) Simmie, J. M.; Somers, K. P. Benchmarking compound methods (CBS-QB3, CBS-APNO, G3, G4, W1BD) against the active thermochemical tables: A Litmus test for cost-effective molecular formation enthalpies. *J. Phys. Chem. A* **2015**, *119*, 7235-7246.

(69) Gilbert, T. M. Tests of the MP2 model and various DFT models in predicting the structures and B-N bond dissociation energies of amine-boranes (X3C)(m)H3-mB-H(CH3)(n)H3-n (X = H, F; m=0-3; n=0-3): Poor preformance of the B3LYP approach for dative B-N bonds. *J. Phys. Chem. A* **2004**, *108*, 2550-2554.

(70) Demirbas, A. Potential applications of renewable energy sources, biomass combustion problems in boiler power systems and combustion related environmental issues. *Prog. Energy Combust. Sci.* **2005**, *31*, 171-192.

(71) Kohse-Höinghaus, K.; Oßwald, P.; Cool, T. A.; Kasper, T.; Hansen, N.; Qi, F.; Westbrook, C. K.; Westmoreland, P. R. Biofuel combustion chemistry: From ethanol to biodiesel. *Angew. Chem. Int. Ed.* **2010**, *49*, 3572-3597.

(72) Zhang, Y.; Zhang, J.; Sheng, C.; Liu, Y.; Zhao, L.; Ding, Q. Quantitative analysis of NO_x reduction in Oxy-coal combustion. *Energy & Fuels* **2011**, *25*, 1146-1152.

(73) Mendiara, T.; Glarborg, P. Ammonia chemistry in oxy-fuel combustion of methane. *Combust. Flame* **2009**, *156*, 1937-1949.

(74) Darvell, L. I.; Jones, J. M.; Gudka, B.; Baxter, X. C.; Saddawi, A.; Williams, A.; Malmgren, A. Combustion properties of some power station biomass fuels. *Fuel* **2010**, *89*, 2881-2890.

(75) Tian, Z.; Li, Y.; Zhang, L.; Glarborg, P.; Qi, F. An experimental and kinetic modeling study of premixed $NH_3/CH_4/O_2$/Ar flames at low pressure. *Combust. Flame* **2009**, *156*, 1413-1426.

(76) Tian, Z.; Li, Y.; Zhang, T.; Zhu, A.; Cui, Z.; Qi, F. An experimental study of low-pressure premixed pyrrole/oxygen/argon flames with tunable synchrotron photoionization. *Combust. Flame* **2007**, *151*, 347-365.

(77) Tian, Z.; Li, Y.; Zhang, T.; Zhu, A.; Qi, F. Identification of combustion intermediates in low-pressure premixed pyridine/oxygen/argon flames. *J. Phys. Chem. A* **2008**, *112*, 13549-13555.

(78) Wang, Z.; Lucassen, A.; Zhang, L.; Yang, J.; Kohse-Höinghaus, K.; Qi, F. Experimental and theoretical studies on decomposition of pyrrolidine. *Proc. Comb. Instit.* **2011**, *33*, 415-423.

(79) Duynslaegher, C.; Jeanmart, H.; Vandooren, J. Flame structure studies of premixed ammonia/hydrogen/oxygen/argon flames: Experimental and numerical investigation. *Proc. Comb. Instit.* **2009**, *32*, 1277-1284.

(80) Zhang, K.; Li, Y.; Yuan, T.; Cai, J.; Glarborg, P.; Qi, F. An experimental and kinetic modeling study of premixed nitromethane flames at low pressure. *Proc. Comb. Instit.* **2011**, *33*, 407-414.

(81) Nau, P.; Seipel, A.; Lucassen, A.; Brockhinke, A.; Kohse-Höinghaus, K. Intermediate species detection in a morpholine flame: contributions to fuel-bound nitrogen conversion from a model biofuel. *Exp. Fluids* **2010**, *49*, 761-773.

(82) Lucassen, A.; Labbe, N.; Westmoreland, P. R.; Kohse-Hoinghaus, K. Combustion chemistry and fuel-nitrogen conversion in a laminar premixed flame of morpholine as a model biofuel. *Combust. Flame* **2011**, *158*, 1647-1666.

TOC